CFD simulation of a simplified model of the Sardinia Radio Telescope

Stage Activities Report

CRS4

July – October 2017

Author

G. Murtas

Coordinators

Vincent Moreau, Manuela Profir

LIST OF CONTENT

Introduction

The main goal of this work is to examine the potentiality of the STAR-CCM+ software for Computational Fluid Dynamics (CFD) when applied to a simplified astronomical analysis. In this framework, the construction of the numerical model of a radio telescope has been realized. The pressure and temperature profiles are inverstigated by simulating the combined effect of the sun and the wind at different speeds on the structure. The geometry of this simplified instrument is based on some of the features of the Sardinia Radio Telescope, a major radio astronomical facility located near San Basilio, in Sardinia, Italy ([1]).

All activities were performed under the careful supervision of Dr. Vincent Moreau in his role of internship tutor and Dr. Manuela Profir, in the *Smart Energy System* research program at the CRS4 (Centro di Ricerca, Sviluppo e Studi Superiori in Sardegna), one of the top-level research centers in Italy located in Sardinia. The main goals of the HPC for Energy and Environment team – particularly the Smart Energy System group – are to employ multi-disciplinary methods for applied research into all energy resources and technologies for industry, households and services, focusing on the numerical modeling of physical phenomena ([2]).

The reporting of the activity follows the classical order of a STAR-CCM+ simulation and the progressive understanding of the numerical model built in the framework of the stage. In

Section 1, the geometrical model is presented. In Section 2, the various mesh models adopted for the discretization of the geometry are described. In section 3, the physical models suitable for the analysis are illustrated. In Section 4, the physics conditions assigned to each region of the model are described. In Section 5 and Section 6, the fluid dynamics analysis and the thermal analysis are performed. Finally, in Section 7, the basic elements of a preliminary thermal stress analysis are given.

1. Geometry

The optical system of the Sardinia Radio Telescope is based on a quasi-Gregorian dish antenna, as shown in detail in Figure 1. The radio telescope is equipped with an active surface made of 1008 panels for the primary mirror and 49 panels for the secondary mirror, which is adjustable with 1116 actuators. Each surface panel, made of aluminum covered by a titanium dioxide based paint, is about 7 mm thick. In a first raw approximation, only the primary and secondary mirrors are simulated as unique surfaces, as well as the receiver located in the primary focus and modeled as a cylindrical shaped block of aluminum.

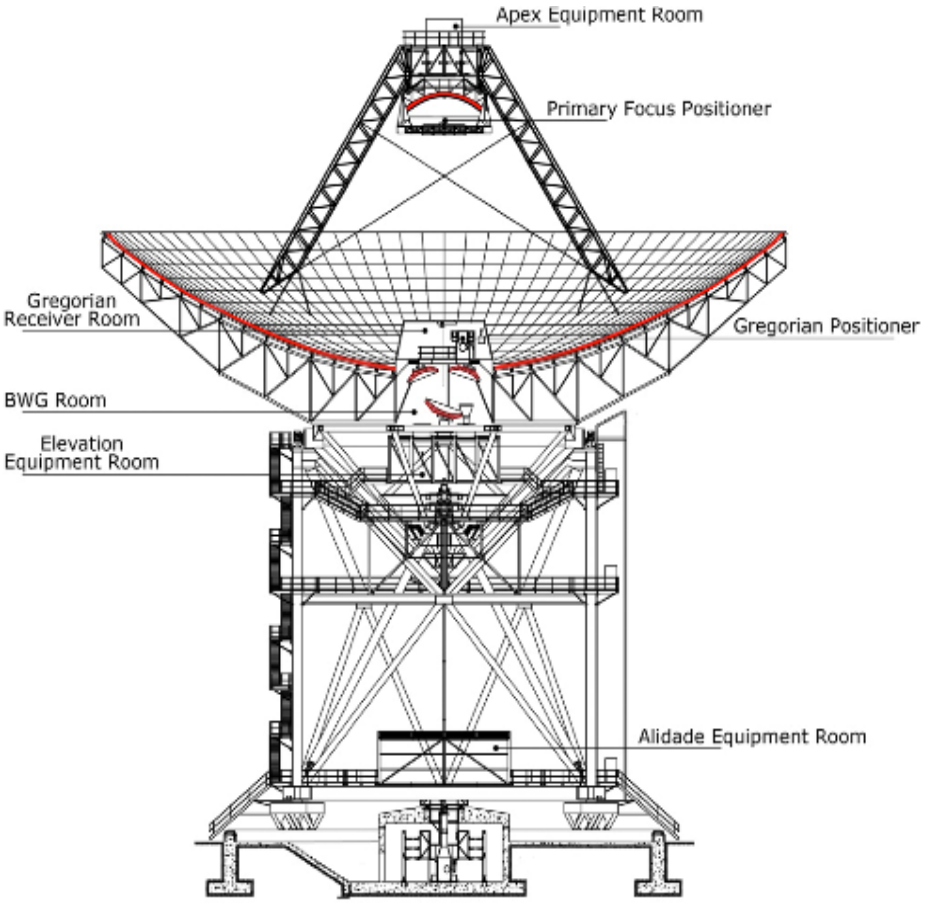

Figure 1 Outline of Sardinia Radio Telescope structure. Credits: SRT/INAF-OAC

The technical features of the simulated structure are listed in Table 1.

Table 1: Length values of the simulated structure

Primary Mirror Diameter (m)	64
Secondary Mirror Diameter (m)	7.9
Mirrors Thickness (m)	0.2
Receiver Radius (m)	0.1
Receiver Height (m)	0.1
Distance from the ground (m)	70

The parabolic shaped mirrors were built by applying a rotation to parabola branches, which were sketched using splines. Splines points were located in precise coordinates through the relation:

1.1 $$4p(y - k) = (x - h)^2$$

where p is the distance between vertex and focus and (h, k) are the vertex coordinates. The origin of the axes in the Laboratory Reference Frame is set at the center of the primary mirror, on the internal surface, and the distance between the internal surfaces is kept constant: defining the mirrors thickness as *Design Parameters*, it is then possible to carry out data collection for different independent thickness values without shifting the position of the primary focus, in which the center of the receiver is located.

The solid structures are immersed into a 70x70x220 m box which would represent the air mass around the telescope. The fluid domain is obtained by subtracting the solid structures from this surrounding box. Such dimensions were chosen in order to set a first limit to computational constraints along the borders, especially at the inlet and outlet surfaces. However, in case of wind simulation, an interaction with the incoming air flux is still observed, together with a noticeable interaction between the structure and the flux moving away from it. To completely avoid these computational constraints, the air box should be enlarged of a distance equal to about five times the primary mirror diameter in both the inlet and outlet directions; moreover, its height should be increased in order to solve an eventual constraint due to the upper box surface. Despite these problems, the flux behavior around the structure can be treated with a significant approximation.

Later in the simulation, a rotation motion has been applied to the antenna system. In order to better perform the rotation, a spherical body, surrounding the mirrors and filled with air, has been added in the 3D-CAD Model. The solid structure is not subtracted anymore from the rectangular box but from this spherical body. The air domain will be constituted by the union of the box air and the sphere air by means of a method which will be explained in detail in the next section. The air sphere radius is 45 m, defined into the *Design Parameters*. The complete geometry of the model is shown in Figure 2.

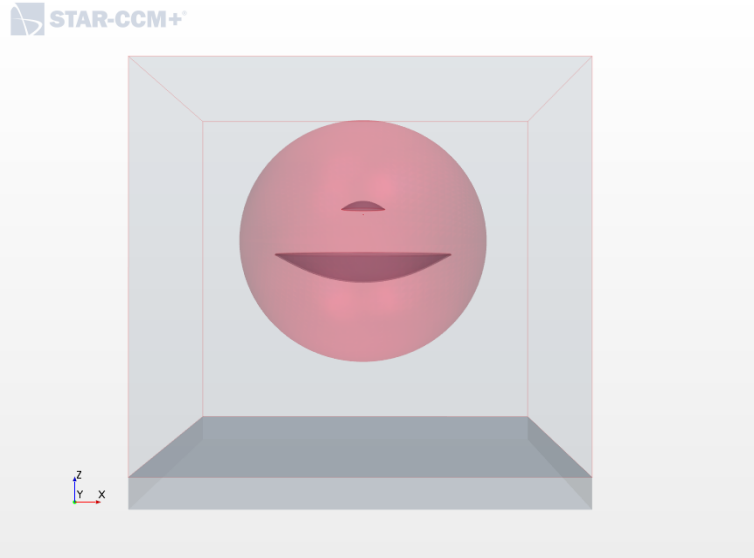

Figure 2 The 3D-CAD model of the antenna system

In view of the meshing operations two Shape Parts, which have no correspondence with a specific body from the 3D-CAD Model, were created. A cylindrical part, set around the receiver, has a radius of 0.15 m and a height of 0.3 m along the z axis. Its position has been defined in a Local Coordinate System centered on the receiver at [0, 0, 25] m. Another spherical part, with a radius of 46 m, is defined and encloses the air sphere.

2. Mesh operations

The geometrical complexity of the model is given by the fact that length measures differ of several orders of magnitude between the small mirrors thickness and their own diameters. For this reason, the geometry requires a proper discretization in order to obtain an optimized numerical solution from the physics solvers. For this aim, four different mesh operations related to two meshing strategies (Automated Mesh and Directed Mesh) were defined.

Mesh operations are completely disconnected from the physical properties of the regions, being defined at a previous level, at the Geometry parts level. Each body may be discretized with a different mesh operation, feature that leads to a considerable advantage in terms of modification simplicity of discretization parameters.

2.1. Automated Mesh

The Automated Mesh operation generates unstructured surface and volume meshes for its input parts, and is allowed to manage all the meshers. In the simulation, this meshing strategy was applied separately to the receiver and the air sphere together in one operation and to the air box in another operation. In both cases, the following meshers were chosen:

- *Surface Remesher*: it retriangulates the surfaces to improve quality discretization that will be used as a base for the volume mesh, and can include localized refinement with respect to curvature and surface proximity;

- *Automatic Surface Repair*: related to the Surface Remesher, it provides an automatic procedure for correcting a range of geometric problems generated from the remeshing process;
- *Polyhedral Mesher*: suitable for heat transfer problems, it leads to a mesh of arbitrary polyhedral-shaped cells and is a faster operation compared to other cell shapes meshers, as it contains fewer cells for a given starting surface;
- *Prism Layer Mesher*: it generates orthogonal prismatic cells next to body surfaces and boundaries (with the exception of inlet and outlet surfaces), which improve the accuracy of the solution in case of flux determination along physical constraints.

The main sizes set for both the automated meshes are listed in Table 2.

Table 2: Values of the relevant mesh sizes

	Receiver/Air Sphere	*Air Box*
Base Size (m)	1	2.5
Target Surface Size (m)	1	2.5
Number of Prism Layers	4	4
Mesh Density	0.5	0.5
Mesh Density Growth Factor	15.0	15.0

Applying mesh operations, the gap between the length orders of magnitude of the mirror diameters and their thickness – as well as with the receiver – was leading to the generation of a considerable number of narrow cells filling the whole space between the mirrors themselves. An optimization has been possible by modifying the Mesh Density parameters, lowering the cell density and increasing the growth factor that changes the rate at which cells grow from coarse to fine areas. In this way, fewer cells were generated as their growth became faster.

In addition to the default operations, specific zones around solid bodies were locally refined by three Surface Control operations – linked to interfaces between air and the mirrors thickness and the receiver surface – and two Volumetric Control operations – associated to the spherical and cylindrical Shape Parts (the latter is shown in Figure 3).

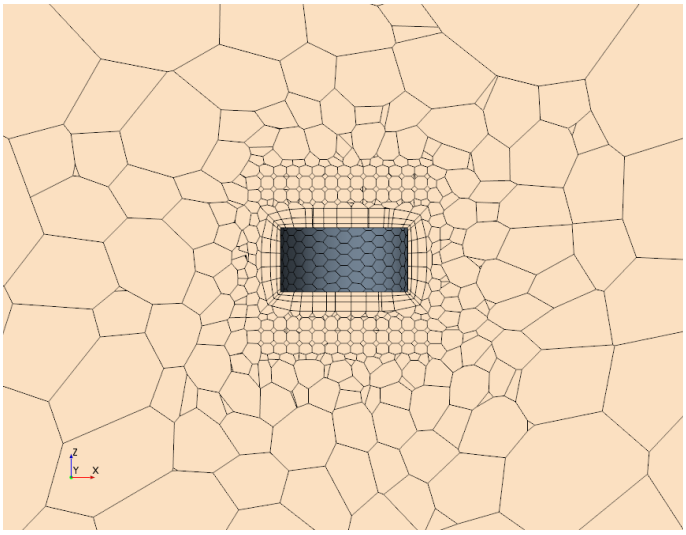

Figure 3 Volumetric Control mesh generated around the receiver

The main parameters associated with these secondary operations are listed below:

- Target Surface Size (*Surface Control with no prism layers*): 0.05 m
- Target Surface Size (*Surface Control at the air interface with mirrors thickness*): 0.2 m
- Custom size (*Volumetric Control around the receiver*): 0.02 m
- Custom size (*Volumetric Control around the air sphere*): 1.5 m

In one of the Surface Control operations above, prism layers were disabled, as the associated part refers to the receiver. No prism layers are in fact generated inside solid bodies, as it is not physically expected to observe a flow.

2.2. Directed Mesh

The Directed Mesh operation generates structured meshes with a high degree of control through a volume, by sweeping a surface mesh onto a facing target surface. This operation has been usefully applied to the discretization of the solid mirrors: in fact, due to their small thickness, standard meshing techniques could not lead to a correct building of multiple cell layers inside the solid bodies. As seen in detail in Figure 4 that shows the primary mirror border, five parallel layers were created for both mirrors. The high number of layers allows then a measure of heat transfer and stress inside solids with a greater accuracy. In both cases the source surface, from which the mesh has been swept through the volume, is the internal mirror surface, while the target surface is the external one. The choice has been made by taking into account the problems that the cell minimum size limit may have caused if the resulting cells on the target surface would have been smaller than the set value.

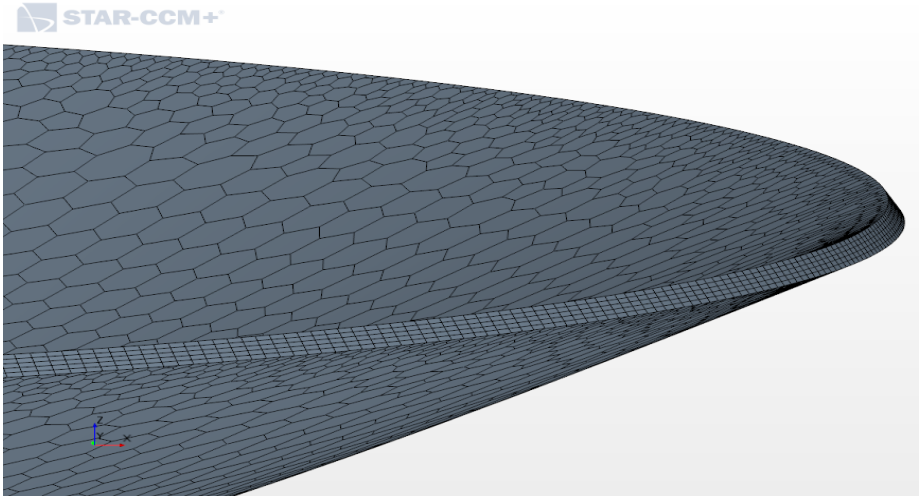

Figure 4 Detail of the discretization applied to the primary mirror with the Directed Mesh operation

The Directed Mesh operation requires a lower generation and calculation time with respect to other meshing techniques. For this reason, this kind of mesh has been also applied to the ground, which has a secondary role inside the simulation and does not need to be discretized

in a high number of cells. For the ground, ten parallel cell layers were built, as shown in Figure 9.

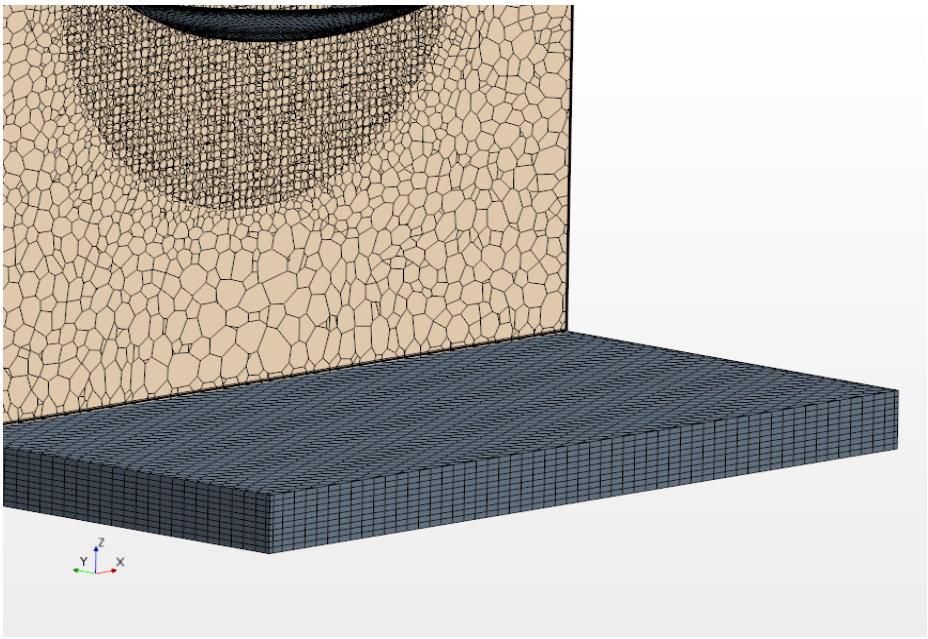

Figure 5 Detail of the ground discretized by means of the Directed Mesh operation

2.3. Overset Mesh

In presence of multiple or moving bodies problems, it is useful to discretize the computational domain by means of overset meshes, namely meshes which overlap each other in an arbitrary manner. The great potentiality of this operation is that, in most cases, no further mesh modifications are required after generating the initial mesh. Standard meshing techniques may in fact limit the possibility of motion because of cells degradation during transient simulations, which leads to the necessity of repeating frequently mesh operations along the simulation.

In every solution in which an overset mesh is used, the computational domain is divided into two main regions: a background region enclosing the entire solution domain, and at least one smaller region containing the physical bodies, which is cut from the background. In this work the air box acquires the role of background region, while the air sphere is the region which surrounds the solid bodies.

The overset region is defined through the creation of an Overset Mesh boundary, which is coupled to the background mesh. The boundary is characterized by an overlapping zone that should contain at least 4-5 cell layers from both the regions. As the physics continuum in the two regions must be the same, the creation of the **Overset Mesh Interface** between them becomes available only once a single continuum is defined and assigned. Moreover, the cells in the overlapping region must be similar in size on the background and overset meshes, to eventually reduce interpolation errors.

The resulting mesh can be visualized in two different ways depending on the chosen representation. When applying the Volume Mesh representation (as illustrated in Figure 6 and Figure 7), a map of the coupled meshes is shown, where the computational domain has been

solved yet for the overlapping region. In Figure 8, where only the air box is taken into account, it can be noticed the cut left by the superposition of the overset mesh. On the other side, the Overset mesh representation shows a map of individual meshes contributions towards the computational domain, as it appears in Figure 7 (where the background contribution appears also in the overset region) and in Figure 9 (referred to the air sphere only).

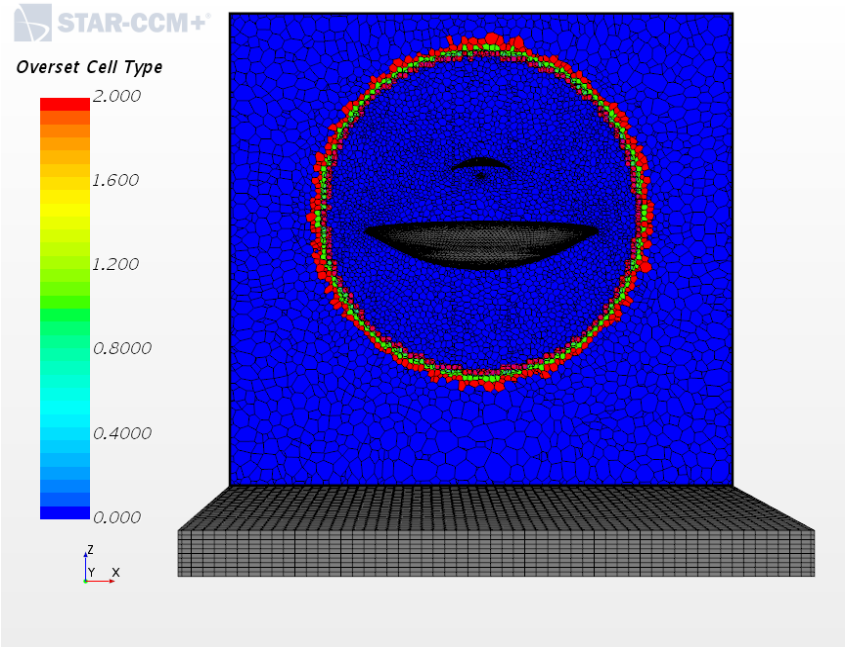

Figure 6 Map of overset cell types in the Volume Mesh representation of the whole computational domain

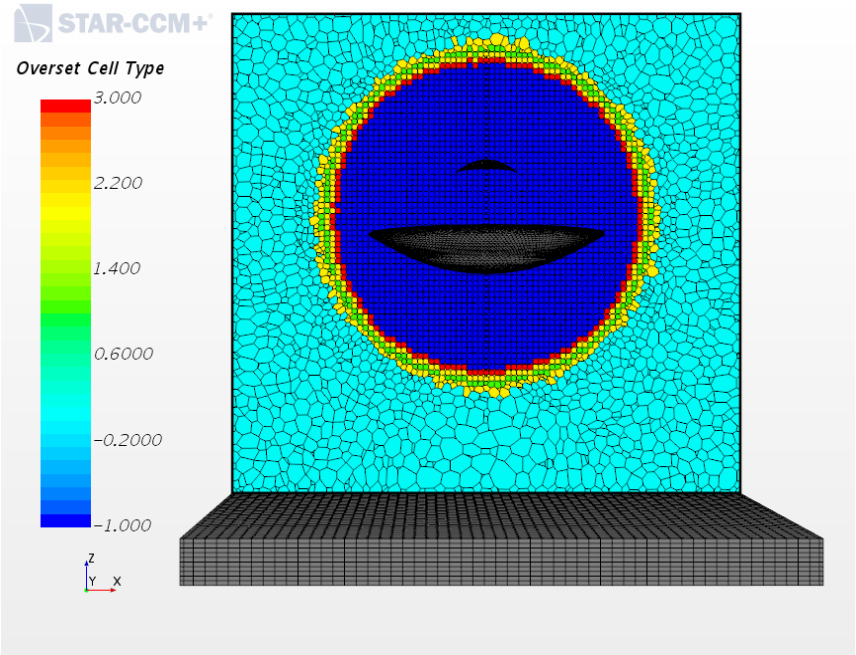

Figure 7 Map of overset cell type in the Overset Mesh representation of the air box (its contribution only)

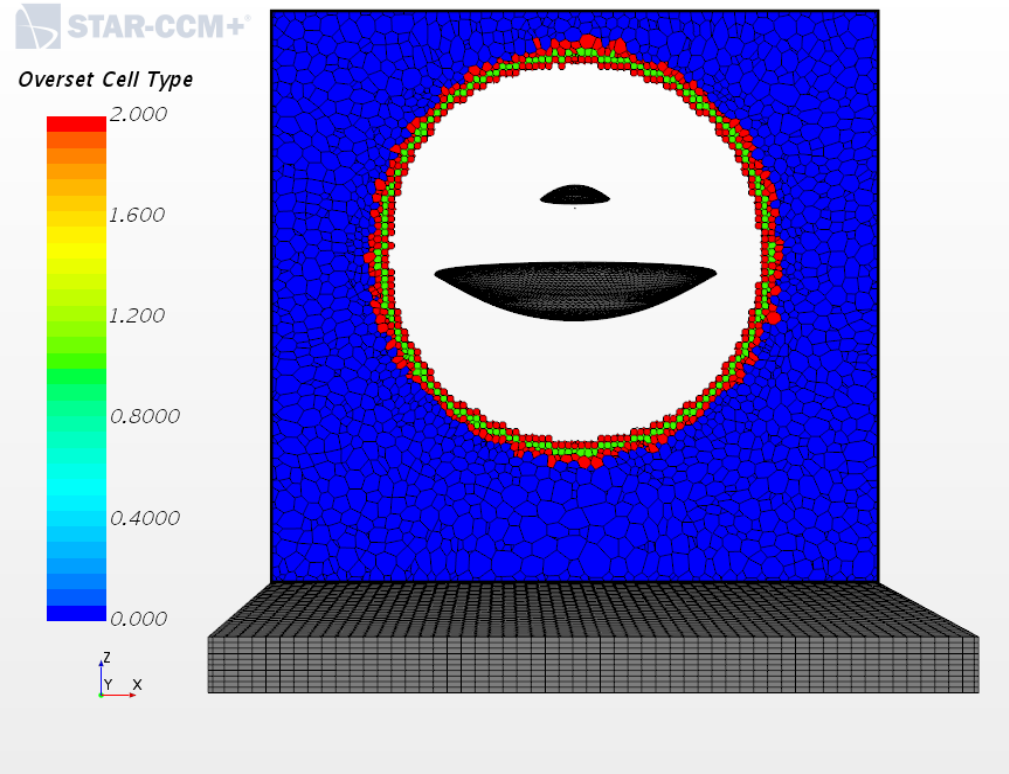

Figure 8 Map of overset cell type in the Volume Mesh representation of the air box

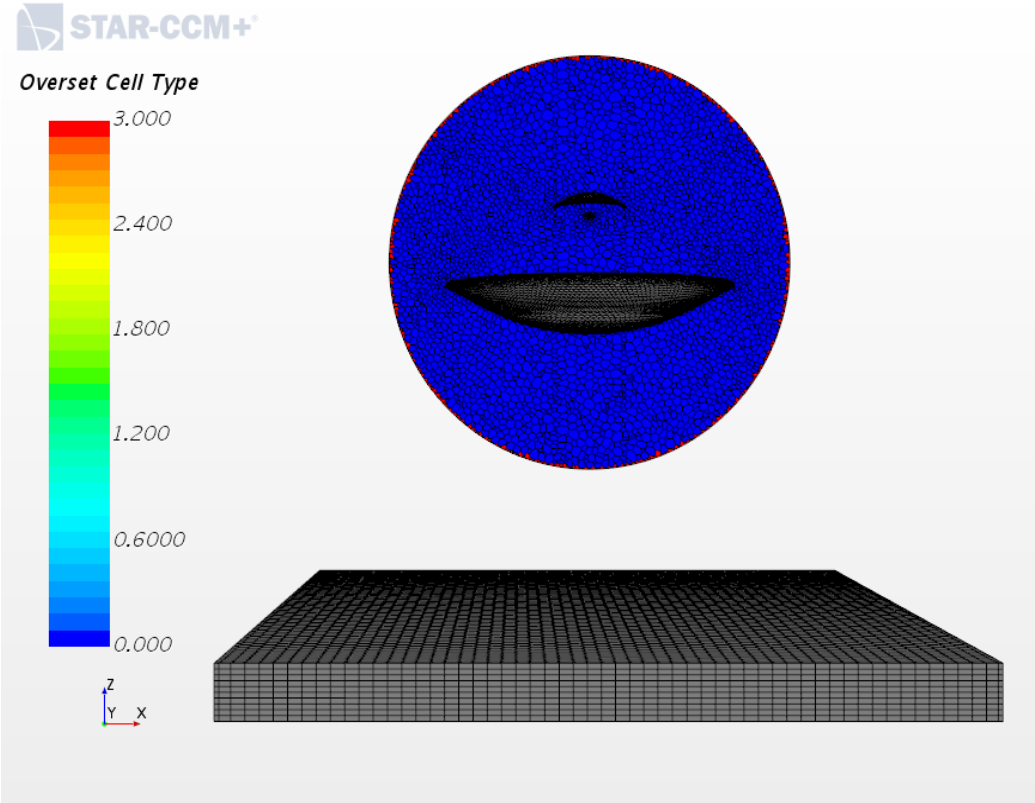

Figure 9 Map of overset cell types in the Overset Mesh representation of the air sphere

3 Physical and mesh continua

The following Section contains the description of the physics models that were applied to the regions in order to simulate the material behavior under the action of several factors. The thermal and physical interaction of our model, as well as the radiation field, requires the representation of three continua: aluminum, air and ground.

3.1 Aluminum modeling

Aluminum is the material associated to the antenna dishes. As a first approximation, the same continuum is also associated to the receiver, which is characterized by optical properties similar to the mirrors ones. The following models were applied to this continuum:

- Three Dimensional
- Solid
- Constant Density
- Segregated Solid Energy
- Gradients
- Cell Quality Remediation
- Steady state

In the first part of the project, the impact of the wind on the antenna was analyzed by considering different speeds of the wind in steady state. Then, for the effective simulation of the system motion, the chosen model for time is Implicit Unsteady.

Material properties are reported in the Solid model, and can be selected from the material database. In particular, aluminum is characterized by the following properties:

- Density (Constant value = 2702 kg/m^3)
- Specific Heat (Constant value= 903 J/kg-K)
- Thermal Conductivity (Constant value= 237 W/m-K)

As mentioned in Table 2, the simulated mirrors thickness assumes a noticeable higher value if compared to the real measure of the panels, because of the limits observed for a proper mesh generation. This discrepancy becomes important once the heat transfer analysis is taken into account. If the goal of the current model is to analyze the results related to 1 cm thick panels, the material properties above can be corrected by a scale length factor that can be calculated from the heat equation:

$$q_x = -\lambda A \frac{\Delta T}{\Delta x} \qquad 3.1.1$$

where q_x is the thermal power of a mono dimensional flux through the surface A, and λ is the thermal conduction coefficient.

In this specific situation, density is divided by a factor of 20, while the thermal conductivity is multiplied by a factor of 20^2 to obtain the heat transfer description from one panel surface to the other along a 1 cm thick aluminum layer.

In the Continua section, other two fields are left to be discussed: Reference Values and Initial Conditions. The Reference Values refers to the constrains applied to the temperature field, and are the following:

- Minimum Allowable Temperature =100 K
- Maximum Allowable Temperature=5000 K

The temperature interval has been left at the default values – with extreme values at the boundaries – in purpose, in order to allow a proper thermal development of the model without any strictly limiting condition.
The Initial Conditions field has the following setting: Static Temperature= 300 K.
The initial Static Temperature field is constant by default, and taken equal to the typical environment temperature. As this is a steady-state simulation, this setting is not a real constraint as the converged solution will be independent of the initial field.

3.2 Air and solar modeling

The antenna mirrors system is hung above the ground at about 70 m, and immersed into a considerable mass of air. The following models were applied to the air continuum:

- Three Dimensional
- Gas
- Constant Density
- Gravity
- Cell Quality Remediation
- Segregated Flow
- Gradients
- Segregated Fluid Temperature
- Turbulent
- Reynolds-Averaged Navier-Stokes
- K-Epsilon Turbulence
- Realizable K-Epsilon Two-Layer
- Exact Wall Distance
- Two-Layer All y+ Wall Treatment

For the thermal and radiation field discussion the following models are considered :

- Radiation
- Surface-to-Surface Radiation
- Gray Thermal Radiation
- View Factor Calculators
- Solar Loads

Among the models that describe the radiation behavior and interaction with the system, only the Surface-to-Surface Radiation *(*S2S Radiation) model allows the use of the *Solar Loads* optional model, which is an important feature for a complete picture of the radiation field generated specifically by the sun. The S2S Radiation model concerns only the radiating and absorbing surfaces, while the medium that fills the space between them is non-participating. This means that the specified radiation properties and the thermal boundary conditions define the amount of radiation received or emitted at a surface.

For both radiation models, two different radiation spectrum descriptions are possible: the Gray Thermal Radiation Model and the Multiband Thermal Radiation Model.

In the framework of this stage, in which attention is focused on the temperature field generated by solar radiation instead of the accurate simulation of the radiation path, the Gray Thermal Radiation Model was taken as good approximation of the solar spectrum. This model simulates diffuse radiation independently, without respect to wavelengths. Using this feature, optical properties are the same for each surface along the whole spectrum.

The Gray Thermal Radiation Model can be characterized by the Thermal Environment feature, which is a simplified representation of the environment surrounding the continuum, from the standpoint of thermal radiation. It is modeled as a black body with unity emissivity, and hence can be characterized solely with the Radiation Temperature feature.

- Thermal Environment (Radiation Temperature = 300 K)

This temperature, left at the default setting, defines the energy that is effectively radiated from the environment: however, since there has to be only one environment, its value must be the same in all continua.

As mentioned before, with the S2S Radiation model it is possible to enable the Solar Loads optional model, in which the solar emissions are considered together with terrestrial emissions within the context of a given spectrum model. When enabled, no additional radiation property specification on boundaries is needed. For the Gray spectrum model, the total solar loads are applied to the single transfer system representing the full-thermal spectrum. The following values are the Manual Specification settings applied in our work:

- Azimuth = 0°
- Altitude = 90°
- Direct Solar Flux = 900 W/m^2
- Diffuse Solar Flux = 100 W/m^2

The global solar flux reaching the ground in the best scenario – a clear sky – is about 1000 W/m^2, with the 90% of this value related to the direct component, while only 10% is diffuse component coming from the surrounding environment. For this reason, the direct and diffuse radiation fluxes have been set to a lower value with respect to the default settings. The geometric direction of the sun is chosen in order to be aligned with the zenith, which is along the positive z direction in the simulation. All the values listed above must be the same in every continuum which is crossed by radiation: this comes from the fact that only one sun, to which all the continua are exposed, can be present. For continua which are opaque to radiation the enabling of this model is not needed.

Material properties for the air are the following:

- Density (Constant value = 1.18415 kg/m^3)
- Dynamic Viscosity (Constant value = 1.85508 · 10^{-5} Pa s)
- Specific Heat (Constant value = 1003.62 J/kg-K)
- Thermal Conductivity (Constant value = 0.0260305 W/m-K)
- Turbulent Prandtl Number (Constant value = 0.9)

3.3 Ground (Concrete)

Concrete is the continuum associated to the ground where the antenna stands. It is simply characterized by the same models that have been used for the aluminum continuum, and it also shares the same Reference Values and Initial Conditions previously depicted. Its material properties are the following:

- Density (Constant value = 2240 kg/m^3)
- Specific Heat (Constant value= 750 J/kg-K)
- Thermal Conductivity (Constant value= 0.53 W/m-K)

The importance of this continuum is related to its optical surface properties, shown in detail in Section 4, which lead to a diffuse contribution to the radiation pattern on the antenna surface.

3.4 Parts Meshes

In this mesh continuum, the regions and the interfaces created in the simulation are listed and it is possible to define the method for mapping solution data between different volume meshes. The chosen method for Interpolation Option is Higher-order stencil, which is recommended for transient analysis. This option maps the solution data from one mesh to another by using a stencil of cells and faces on the original mesh. It provides a smoother interpolation compared to the other option (Nearest neighbor) which is quicker and maps the solution data from one mesh to another by comparing the cell centroids in each mesh (the new cell gets the solution data from an old cell whose cell centroid is closest to its own).

4 Regions and boundary conditions

This Section contains the detailed description of the properties set to the bodies which are involved in the model, divided into three main categories: Boundaries, Physics Conditions and Physics Values. The attention is particularly focused on the optical properties of surfaces that define the radiation and thermal field of our interest, as well as the physical properties playing a role in the pressure field analysis.

4.1 Solid regions

The main setting related to the interaction between different continua are given in the Boundaries section. Boundaries are the elements (surfaces or lines) that define the space a region fills by surrounding it. They are created by volume or surface mesh import, interface creation and boundary splitting, and can be of various types. From boundaries, interfaces must be created between different regions, in order to allow the transfer of the appropriate physical quantities during the calculation. This involves creating a so-called "in-place interface" between the wall boundaries enclosing each of the two regions, and then defining this interface as being of an appropriate "contact" type, for example for fluid-solid heat transfer. The following options are applied for all the boundaries of solid elements. The proper boundaries are set as Wall boundaries, while the boundaries interfaces are set as Mapped Contact Boundary.
The thermal physics condition of the wall boundaries is Adiabatic. The receiver is the only solid body for which a single boundary, covering its whole surface, appears. For both mirrors, the boundaries are split into three parts, related to the internal dish surface, the external dish surface and the side area. Boundaries are split also for the ground, for which there is a surface boundary in contact with the air box, an underground boundary and a lateral area unifying the four sides between the two surfaces.

The Physics Conditions section is related to the following features, involving mostly the definition of physics sources of various nature inside the region:

- Convective Velocity Option (None)
- Energy Source Option (None)
- Initial Condition Option (Use Continuum Values)

Convective Velocity Option can be used to specify convective velocity in solid regions, which is not our case. Energy Source Option allows the user to insert a heat source (volumetric, total or specific heat source) inside of the solid region: even this one is not our goal, so the option *None* is chosen.

The last section, Physics Values, refers mainly to the orientation and eventual motion of the region. By default, the Motion Specification is set to Stationary.

In case of a transient analysis, which involves also a rotation motion of the antenna system, the option for Motion Specification is set to Rotation, which has been previously built at the Motions Tools level.

4.2 Fluid regions

In the regions representing the air surrounding the solid structures, which are transparent to radiation, optical properties of surfaces like Emissivity and Reflectivity can now be added at the boundaries. All the settings should be specified inside the fluid-solid interfaces at each Interface [Interface #] boundary – not the Interface boundary – as the latter became defunct once the interface is created. As in the previous case of solid regions, all boundaries of the air sphere are taken as walls, and all interfaces with mirrors and receivers are of Type Mapped Contact Boundary. Conditions for wind flux and solar heat flux can be set for simulation in the

air box, which is the outer region.

For the air box, seven different boundaries are defined. Among them, only one is an Interface [Interface #] boundary, and is set at the interface with the ground, that is the only solid in contact with this region. Its boundaries show the features listed below.

1. Physics Conditions of the Top boundary (Type: Wall):
   - Custom Patch Angularity Specification (Use Region Values)
   - Custom Patch Specification (Use Region Values)
   - Dynamic Overset Behavior (Allowable Overset Face States = Active, Inactive)
   - Radiation Flux Option (No flux)
   - Reference Frame Specification (Region Reference Frame)
   - Shear Stress Specification (No-Slip)
   - Specularity Option (Diffuse Reflection)
   - Tangential Velocity Specification (Fixed)
   - Thermal Specification (Adiabatic)
   - Wall Surface Specification (Smooth)

Even if solar radiation should enter from this boundary, Radiation Flux Option is set to No Flux, as the average radiation field surrounding the system is brought directly by the Solar Loads model. Specularity Option is set to Diffuse Radiation as this boundary should not reflect radiation along a determined direction.

2. Physics Values of the Top boundary (Type: Wall):
   - Blended Wall Function (E = 9; Kappa = 0.42)
   - Surface Emissivity (Constant value = 0.0)
   - Surface Reflectivity (Constant value = 0.0)
   - Surface Transmissivity (Constant value = 1.0)

The sum of surface Emissivity, Reflectivity and Transmissivity must be equal to 1. In order to achieve this result, Reflectivity is usually set to the option Auto Calculate, while the other two factors are set constant. For this boundary, Transmissivity has been set equal to one in order to simulate a continuum medium filling space beyond the simulated region. As the Kirchhoff Law option is enabled, Emissivity is equal to the absorption coefficient.

The features listed above are identical for other two lateral wall boundaries (Wall 1, Wall 2), and similar to the Ground (type Wall) boundary. The are two main differences with the latter. One comes from the Specularity Option selection in Physics Conditions, which is set as Adjustable Reflection Specularity and leads to the presence of a fourth feature in the Physics Values section. The second one comes from the setting of Wall Surface Specification to Rough: this option enables the Roughness Height node in Physics Values, which will have a role in modeling the wind for the fluid dynamics analysis.

3. Physics Values of Ground (Type: Wall):
   - Reflection Specularity (Constant value = 0.01)
   - Roughness Height (Constant value = 0.3 m)

- Surface Emissivity (Constant value = 0.04)
- Surface Reflectivity (Method = Auto Calculate)
- Surface Transmissivity (Constant value = 0.36)

Identical values are chosen for the Ground [Interface] boundary. The surface optical properties are chosen in order to simulate its low reflectivity component which must be added to the diffuse radiation of the system. All the elements should be chosen in order to achieve a reflectivity of about 0.6, which is a proper value for concrete. Transmissivity should be set to zero as the ground is an opaque component, leading to an emissivity value of 0.4. However, the quite high value for emissivity leads to an unrealistic situation during the application of thermal solvers, as the concrete reaches temperatures higher than 150°C. It seems then that the more the absorption coefficient (then the emissivity) is high, the more the temperature increases out of control. No solution is available by modifying the Thermal Specification Option, setting it to Environment or Temperature on the boundaries at the interface, nor setting a lower temperature at the bottom of the solid and maintaining the other boundaries Adiabatic option in order to compensate the higher temperature. The only way to achieve a reasonable value for ground temperature has then been enhancing the material transmissivity and dramatically reducing the emissivity value. This approximation is however acceptable, as the ground characterization importance concerns the reflectivity component only, which affects the antenna radiation environment.

The remaining boundaries are the ones related to the wind and radiation path features, so several features are peculiar of their role, although some other are identical. The settings for the inlet and outlet boundaries which differ from the above discussion appear below.

4. Physics Conditions of Velocity Inlet boundary:
   - Flow Direction Specification (Boundary-Normal)
   - Turbulence Specification (Intensity + Viscosity Ratio)
   - Velocity Specification (Magnitude + Direction)

The radiation thermal properties at this boundary can be eventually set in the Physics Values section with the Radiation Temperature feature.

5. Physics Values of Velocity Inlet boundary:
   - Radiation Temperature (Constant value = 300 K)
   - Static Temperature (Constant value = 300 K)
   - Surface Emissivity (Constant value = 0.0)
   - Surface Reflectivity (Method = Auto Calculate)
   - Surface Transmissivity (Constant value = 1.0)
   - Turbulence Intensity (Constant value = 0.01)
   - Turbulent Viscosity Ratio (Constant value = 10.0)
   - Velocity Magnitude (Constant value = 3.0 m/s)

The main thermal analysis is carried on with a low wind velocity magnitude of 3 m/s, corresponding to a speed of 10.8 km/h, which is far from the real structure constraint of 70

km/h. However, for the pressure field analysis, a second wind speed of 10 m/s has been applied at this level in order to enhance the differences.

6. Physics Conditions of Outlet (Type: Pressure Outlet):
    - Back flow Specification (Direction = Boundary-Normal; Pressure =Environmental)
    - Pressure Outlet Option (constant value = 0.0 Pa)
    - Turbulence Specification (Intensity + Viscosity Ratio)

Pressure Outlet Option simply provides a range of options for constraining pressure on an outflow boundary.

In the matter of the air sphere region, in which all the interfaces with the solid parts of the antenna are defined, the properties set at the boundary are identical to the ones listed above for the Up boundary of the air box. The only exception is, for the Physics Conditions node, the Specularity Option set to Adjustable reflection specularity, which leads to the Reflection Specularity node definition (constant value = 0.05) in Physics Values. Reflection Specularity adds a major control on the optical properties description, as it allows to select the specular fraction of the surface reflectivity: a value of 1, for example, denotes that all of the reflection is specular. The chosen value for this option is 0.05, in agreement with the real efficiency of the Sardinia Radio Telescope.

The other optical properties were modeled from the typical values of a titanium dioxide based paint (which reflectivity is ≥ 0.9). Emissivity has been set equal to 0.1, resulting in a reflectivity of 0.9. As the medium is opaque, transmissivity has been set equal to 0.

The Physics Conditions associated to the air regions contains:

- Patch Specification (Proportion of Faces)
- Internal Radiation Transfer Enabled

In both these regions, Internal Radiation Transfer is enabled due to the transparency of the medium in which the radiation travels. No other sources of energy, mass, momentum and turbulence are added, as wind and solar heat have been defined at the boundaries.

5 Fluid dynamics analysis and results

In the first part of the simulation the system has been given a rotational motion. A rotation motion has been defined in the Tools section, and was applied to the three bodies of the antenna system as well as to the air sphere. The rotation rate set for the simulation is of 0.5 rpm; this value is actually higher than the maximum rotation rates of the Sardinia Radio Telescope, which reaches 0.85°/s (0.14 rpm) for the motion along the azimuth, and 0.5°/s (0.08 rpm) for the motion along the elevation. The rotation axis has its origin at [0.0, 0.0, 0.0] m – at the internal surface vertex of the primary mirror – and is aligned with the [0.5, 0.0, 1.0] m direction.

The pressure field and the air velocity field have been recorded for two different wind speeds of 3 m/s and 10 m/s during the simulation of the rotation.

5.1 Atmospheric Boundary Layers modeling

An useful tool in simulating weather features – i.e. the wind – is given by the ABL (Atmospheric Boundary Layer) modeling, which represents the bottom atmospheric layer in contact with the ground surface. In this region, the air flow interacts with the surface and slows down, while turbulent motions are created by frictional effects and temperature.

A first direct way to model the ABL is to operate on the wall roughness parameters, which can be edited as a consequence of the No-Slip option activation in Shear Specification. The main parameter that has been modified at the ground is the Roughness Height: to enhance the interaction, this parameter is set at 30 cm. On the opposite, the mirrors and receiver surfaces have been taken smooth.

5.2 Velocity and pressure fields

Two transient simulations have been set up and run with two different wind velocities and the antenna undergoing the rotation motion. No thermal specification is foreseen in these cases. The following sets of images illustrate the vectorial velocity field and the pressure field of the system subject to a 3 m/s wind (Figure 10) and a 10 m/s wind (Figure 11).

The full set of images retrieved from the simulations have been successively converted in suggestive animations. The turbulent motion near the ground, related to the surface roughness, is present, even though restricted to a small layer. This is an apparent effect, generated by the considerable dimensions of the system compared to the roughness height.

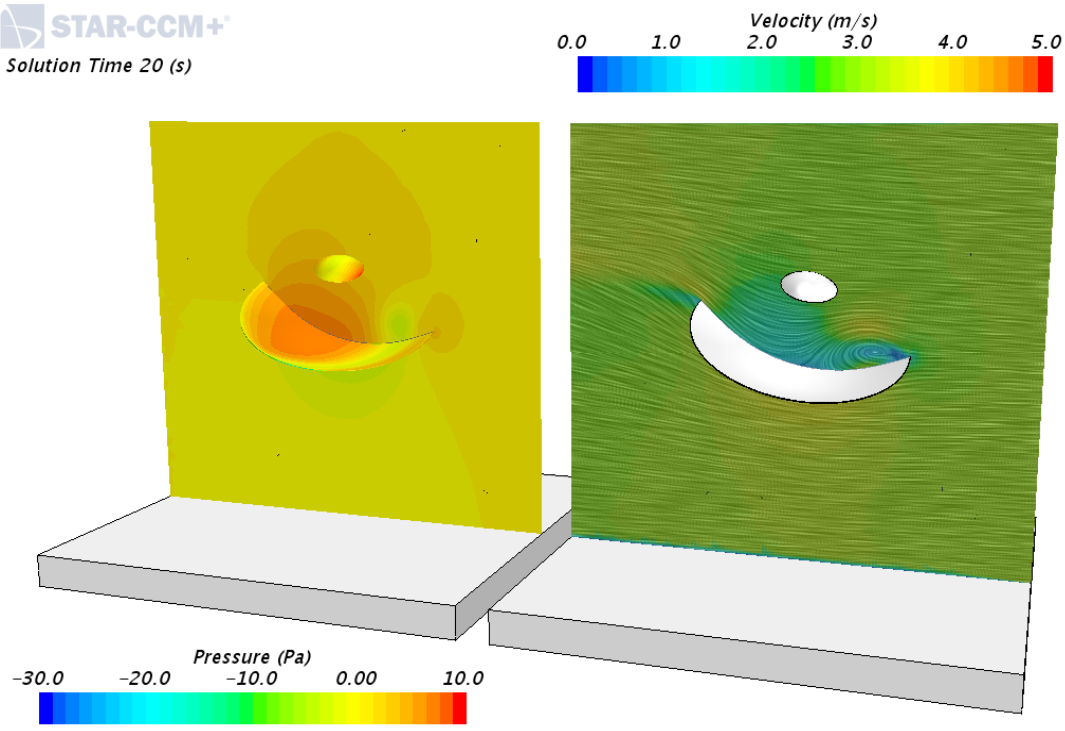

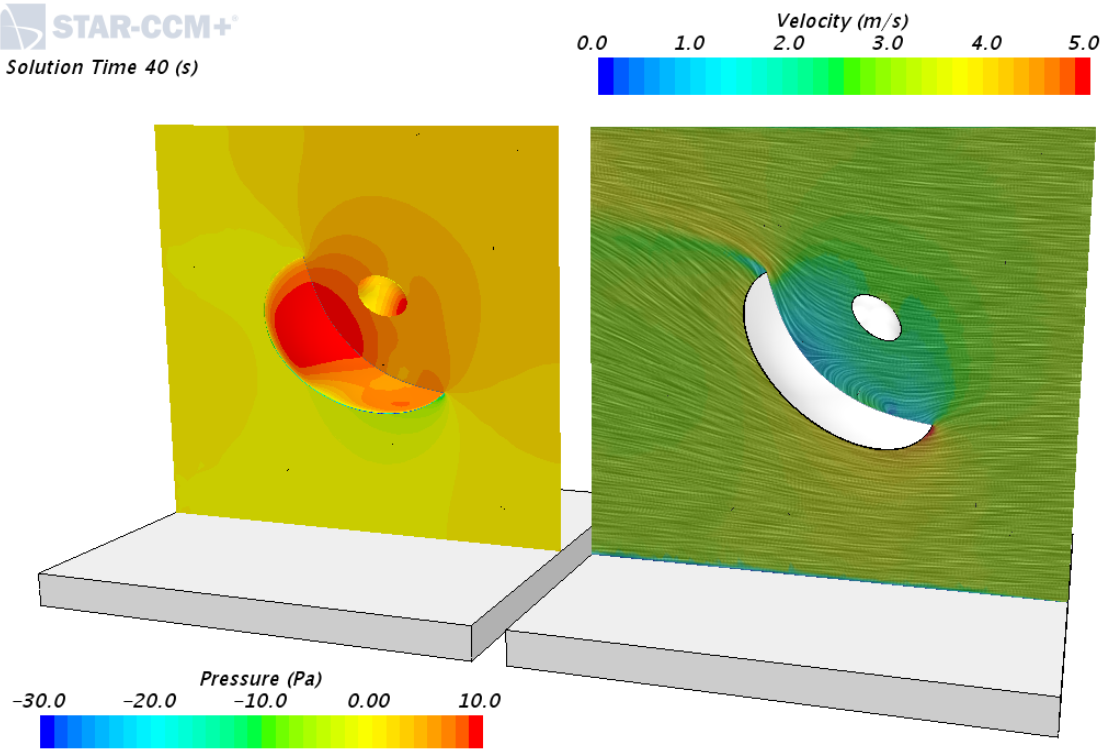
STAR-CCM+
Solution Time 40 (s)
Velocity (m/s)
0.0 1.0 2.0 3.0 4.0 5.0
Pressure (Pa)
−30.0 −20.0 −10.0 0.00 10.0

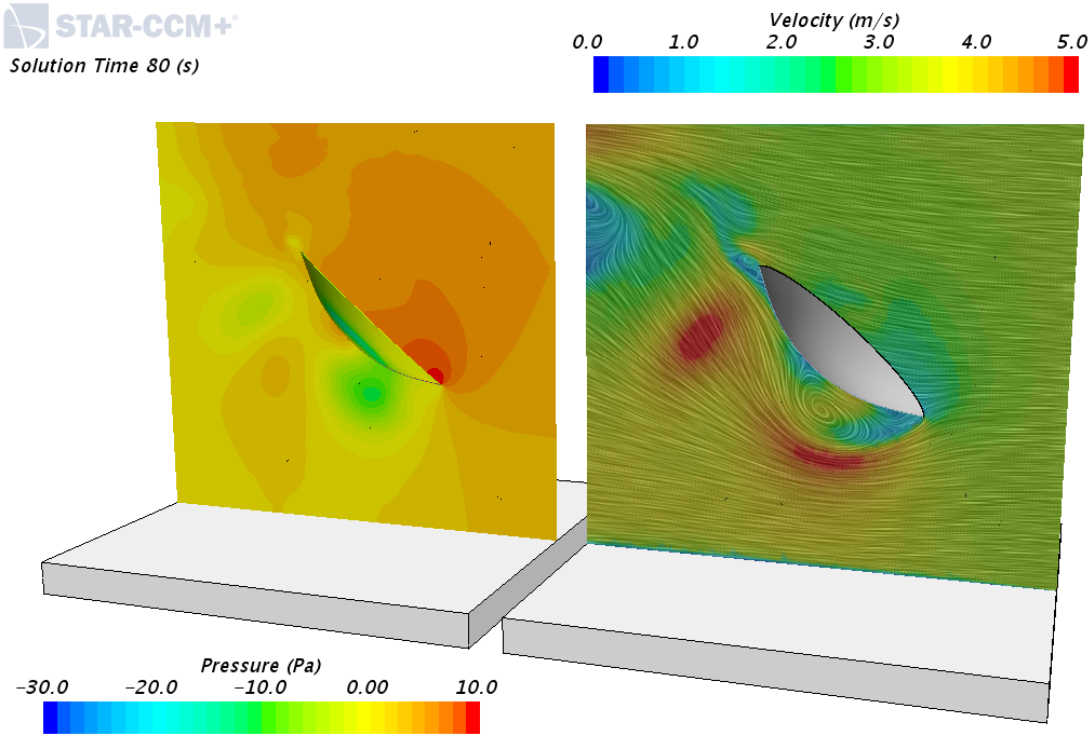
STAR-CCM+
Solution Time 80 (s)
Velocity (m/s)
0.0 1.0 2.0 3.0 4.0 5.0
Pressure (Pa)
−30.0 −20.0 −10.0 0.00 10.0

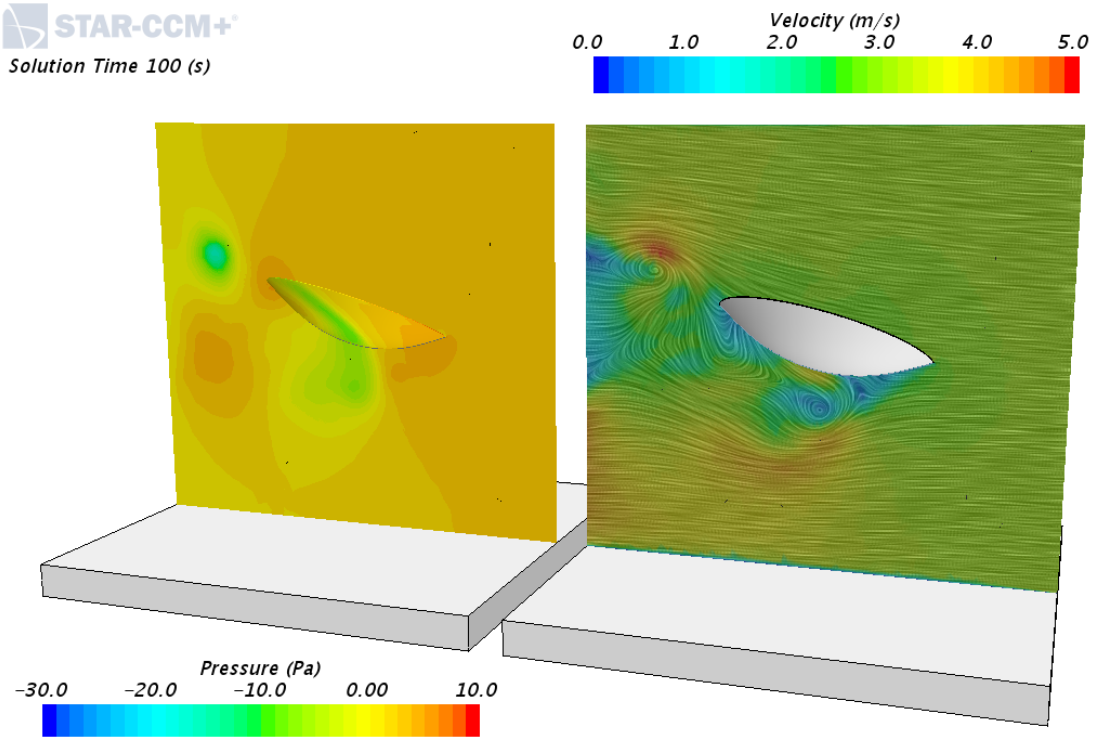

Figure 10 Pressure and velocity field of the system at 3 m/s

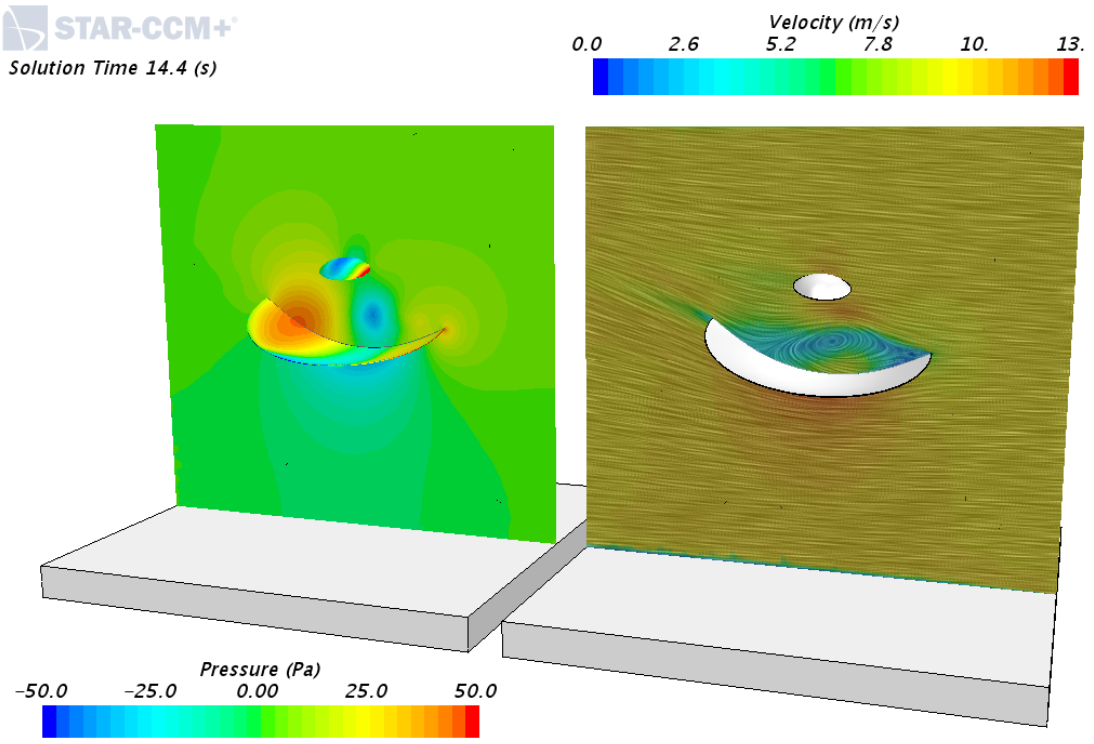

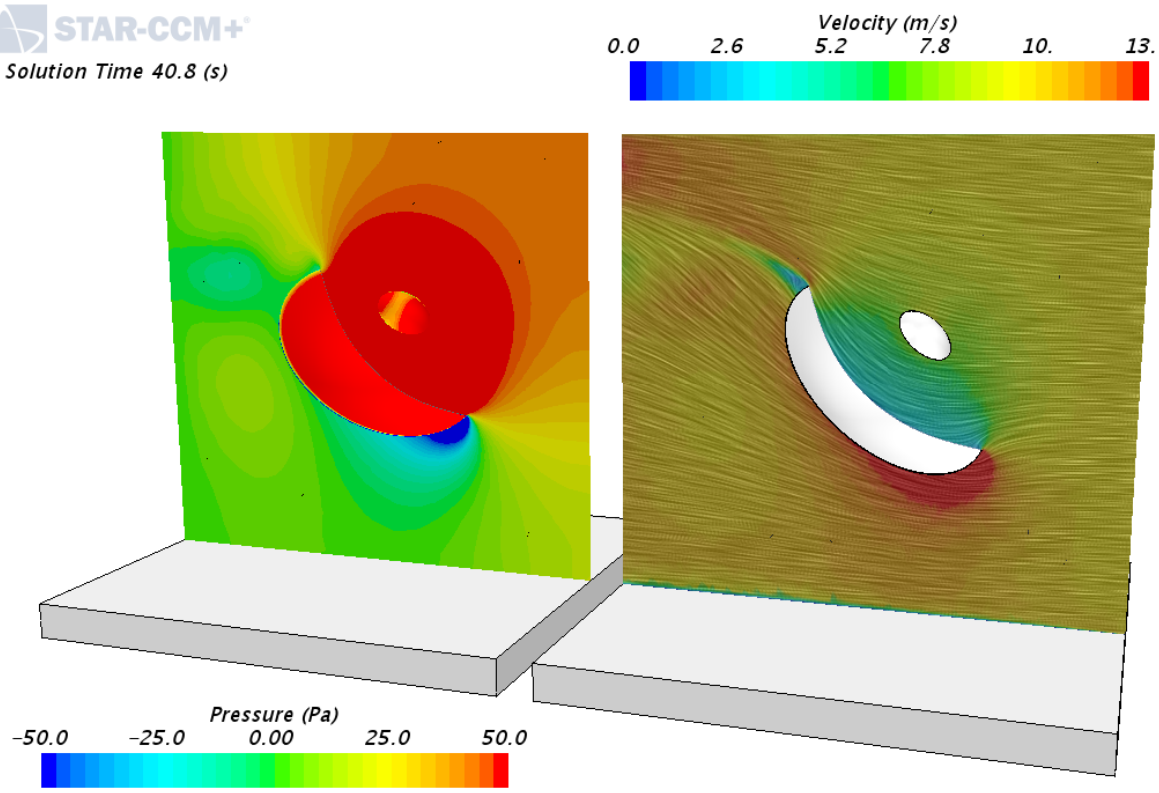
STAR-CCM+
Solution Time 40.8 (s)
Velocity (m/s)
0.0
2.6
5.2
7.8
10.
13.
Pressure (Pa)
−50.0
−25.0
0.00
25.0
50.0

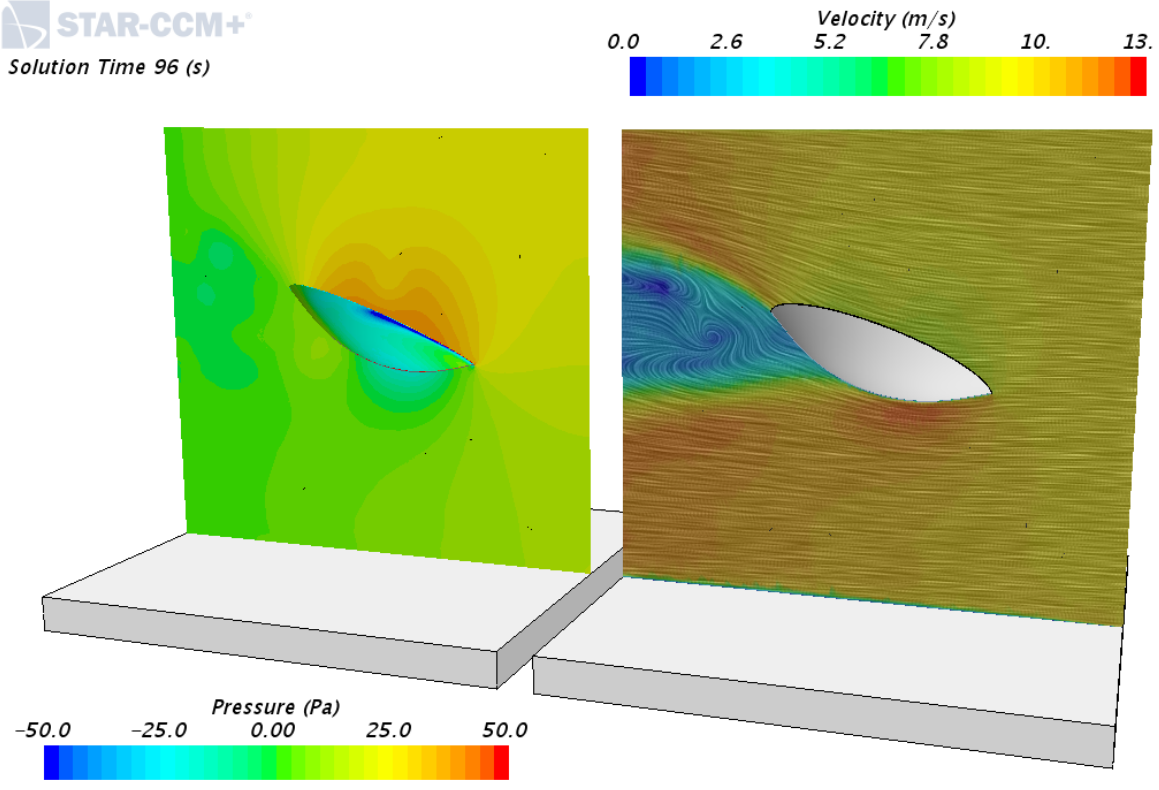
STAR-CCM+
Solution Time 96 (s)
Velocity (m/s)
0.0
2.6
5.2
7.8
10.
13.
Pressure (Pa)
−50.0
−25.0
0.00
25.0
50.0

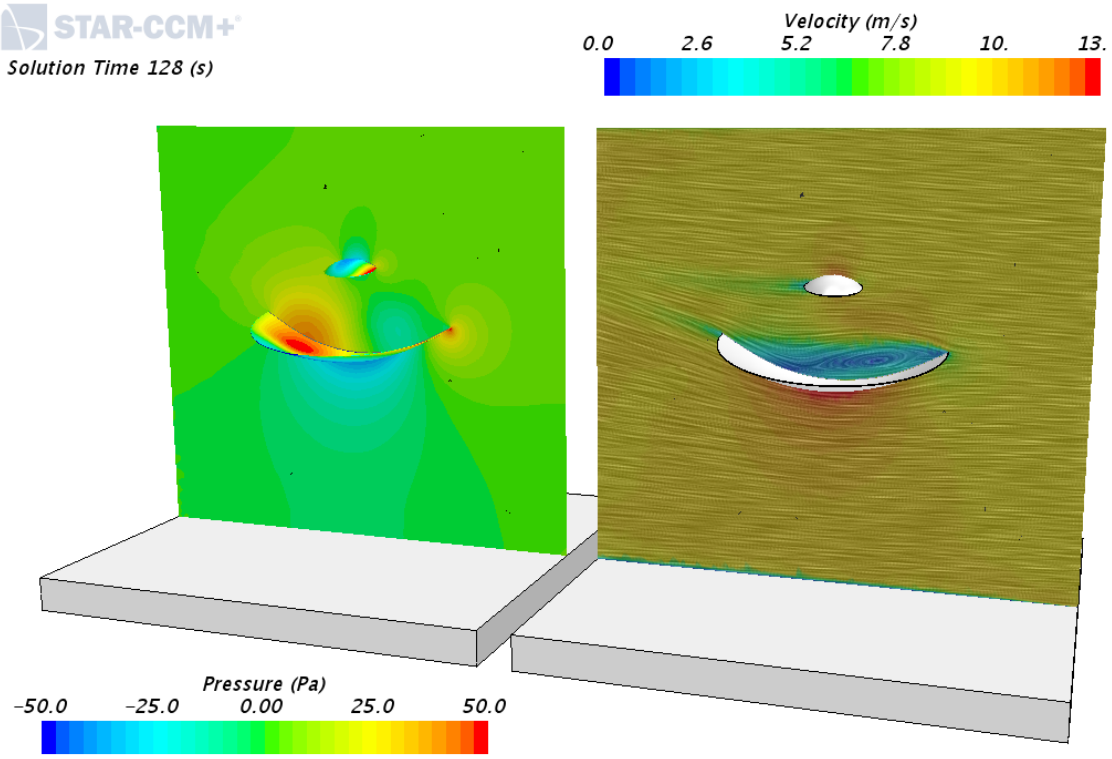

Figure 11 Pressure and velocity field of the system at 10 m/s

6 Thermal analysis and results

The analysis described in this section is focused on the system behavior when inserted into a thermal environment. A tutorial exercise – *Surface-to-Surface Radiation: Thermal Insulator* – was performed as guideline for the Surface-to-Surface Radiation model application. The tutorial example was particularly useful to better understand the suitable settings to define at the boundaries and initial conditions sections. A second tutorial, *Multiband Surface-to-Surface Radiation: Solar Collector*, was analyzed for the Solar Loads model properties.

Three configurations were investigated. Two of them were differentiated by setting the Sun's position at different altitudes: in the first one, the Sun assumes an elevation of 70° with respect to the horizon, while for the second one the Sun is located at the zenith. The third configuration was set by fixing the Sun's position at the zenith and rotating the antenna of 45° along the y-axis, in order to partially orientate the internal surface of the primary mirror towards the direction of the incoming wind. In all the cases, the temperature field was stabilized with an inlet wind velocity fixed at 3 m/s.

The radiation fields generated by the diffuse and direct component of solar irradiation are shown below in Figure 12 and Figure 13. Taking into account the two configurations in which the antenna axis is aligned with the z-axis, the direct solar irradiation field shows the most noticeable difference from one configuration to the other, in particular related to the radiation field intensity and the shadow position. The diffuse radiation field, linked to the environment contribution, is identical for both the Sun's positions.

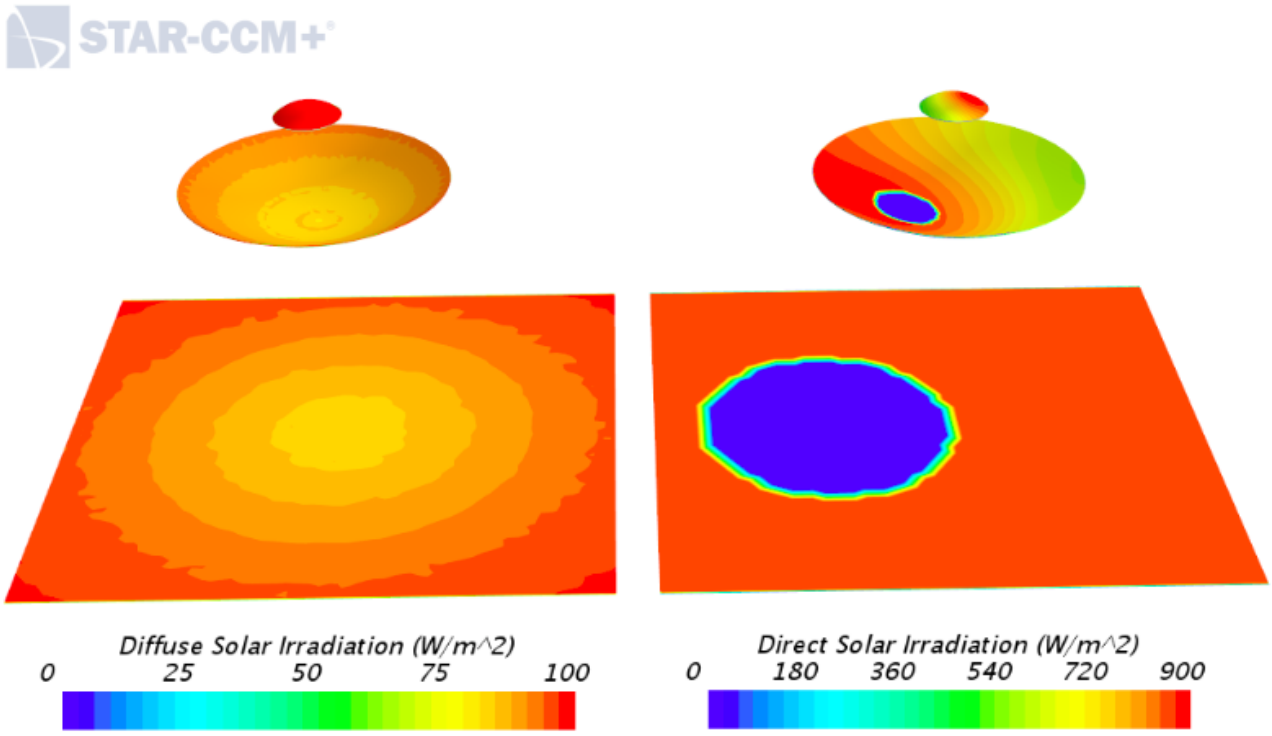

Figure 12 Diffuse and direct contributions of solar irradiation for Sun's altitude at 70°.

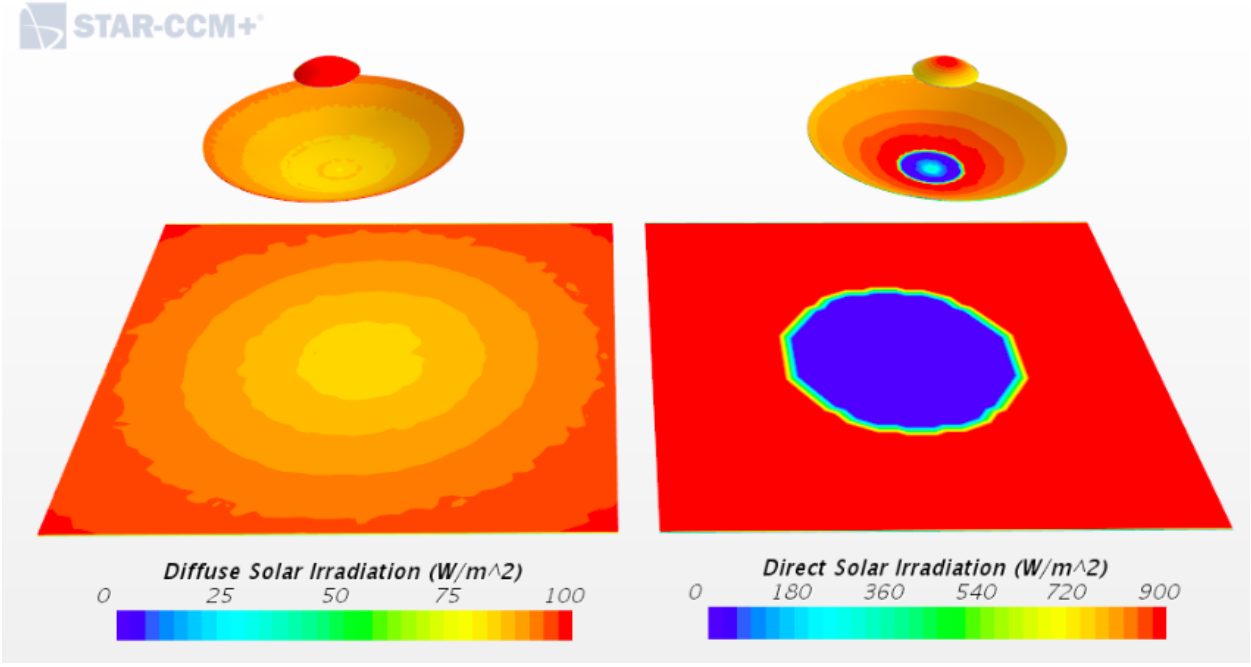

Figure 13 Diffuse and direct contributions of solar irradiation for Sun's altitude at the zenith (90°)

While for the direct solar irradiation there is no flux on the bottom side of the mirrors, for the diffuse irradiation a considerable contribution is originated by the reflection at the ground (on

the external surface of the primary mirror) and at the internal surface of the primary mirror (reflecting on the internal surface of the secondary mirror), as shown in Figure 14.

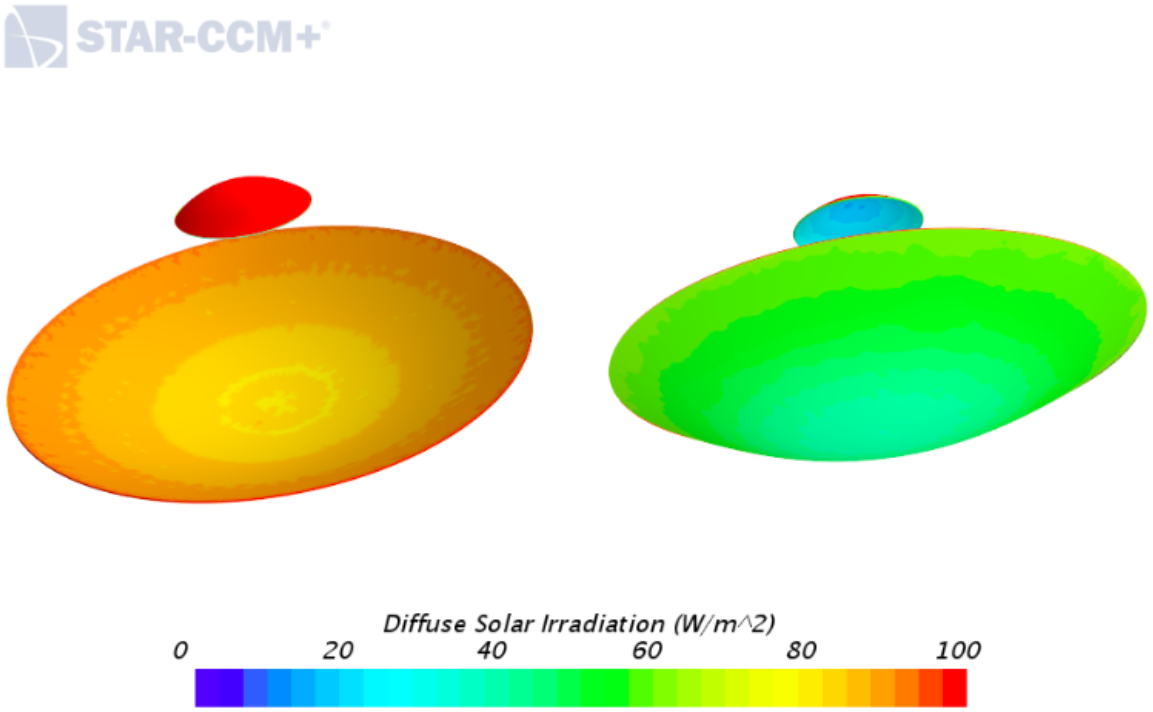

Figure 14 Diffuse solar irradiation flux on the internal and external surfaces of the mirrors

The radiation field observed for the third configuration – in which the Sun is at the zenith and the antenna is rotated – is shown in Figure 15.

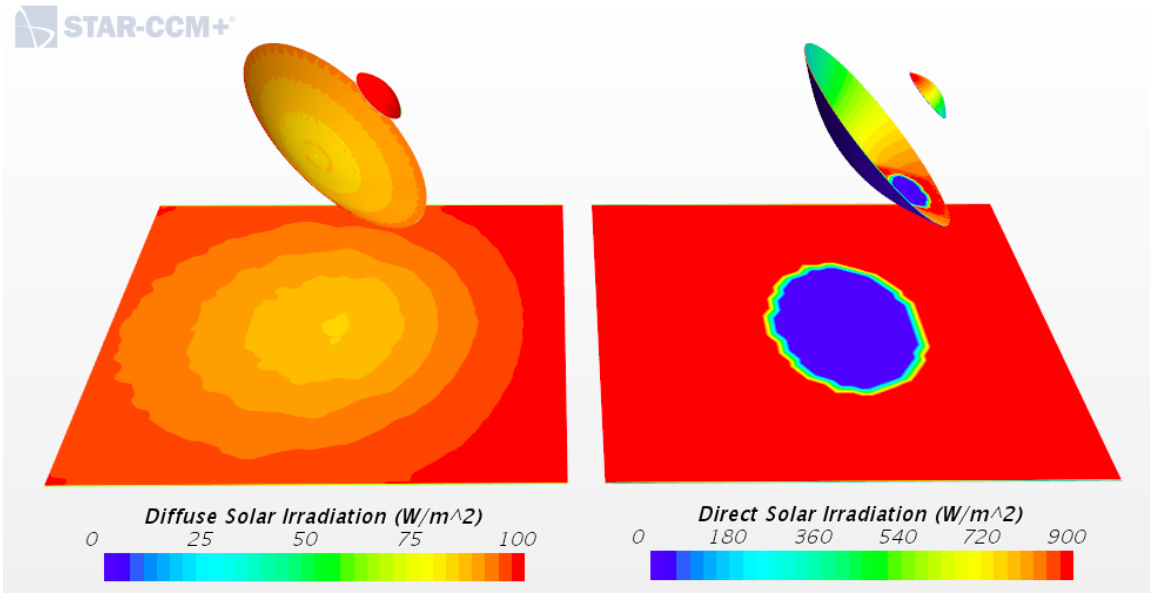

Figure 15 Diffuse and direct contributions of solar irradiation for the antenna at 45° with respect to the Sun's position (zenith)

6.1 Solar position at 70° of altitude

The thermal features of the model – temperature field and heat flux between solid and air – were analyzed after running the thermal simulation for 21000 iterations, in order to achieve the steady state solution. The temperature field is shown in Figure 16.

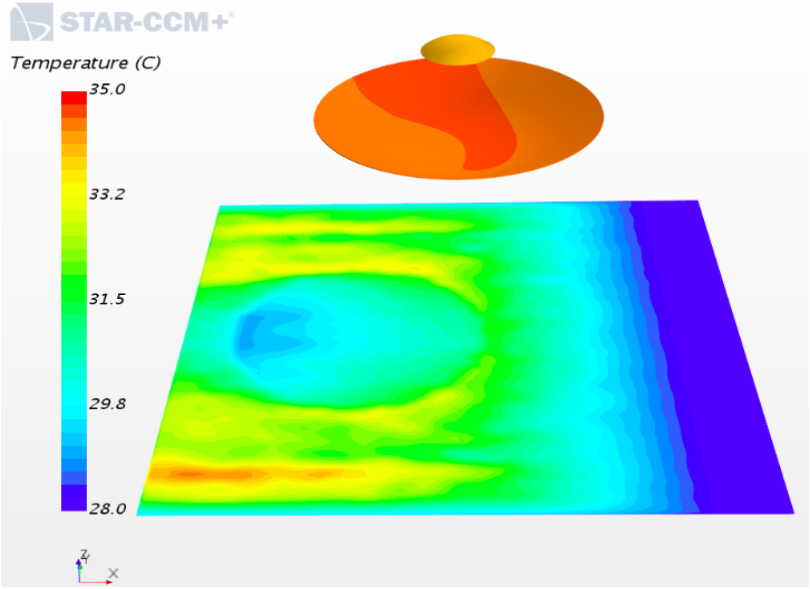

Figure 16 Temperature field of the system for a wind of 3 m/s and a Sun's altitude of 70°

Monitoring the trend of the temperature of the antenna parts (mirrors and receiver), it is possible to verify the convergence of the solution. As shown in the plots in Figure 17, the curves of the maximum temperature gradually reduce their slope with respect to the increasing number of iterations, approaching to a constant value.

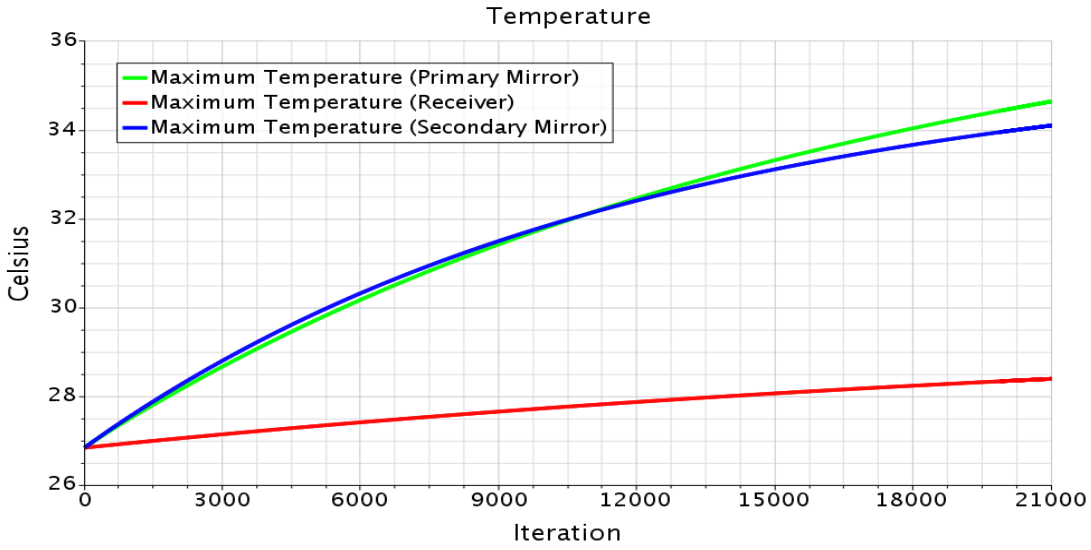

Figure 17 Trend of the temperature of solids (wind at 3 m/s, Sun's altitude at 70°)

The higher temperature at the end of the iterations is achieved by the primary mirror, followed by the secondary mirror and the receiver, which may indicate a dependency on the surface area. In the left part of the graph, the secondary mirror shows a slightly higher temperature, probably related to the initial greater exposure to the direct solar irradiation.

As seen from the curves trend, the Sun's irradiation causes a restrained temperature increase, which does not exceed 10 degrees for both mirrors and it is even more limited for the receiver (that is shielded by the secondary mirror above). This result is compatible with the expected temperature for the real antenna panels, and is constrained by the air flow that provides an important contribution in cooling the system.

In Figure 18 the heat fluxes from solids to the air are shown. In a steady simulation, when the system reaches stabilization, the fluxes decreases towards lower values, eventually compatibles with a null value. This is the trend observed for our system in the limited number of iterations of simulation run.

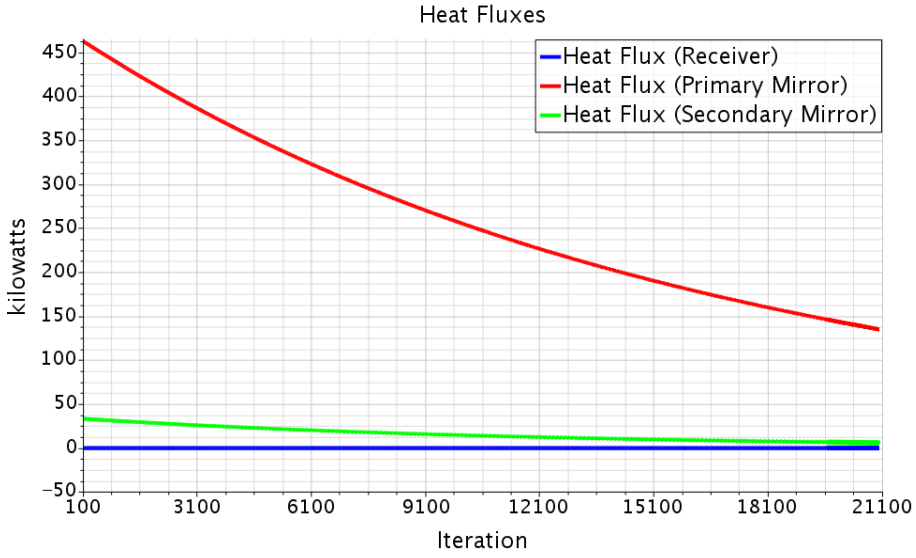

Figure 18 Heat flux from the solid parts of the antenna to the air mass (wind at 3 m/s, Sun's altitude at 70°)

In Figure 19 the heat balance is also reported. This is the net heat flux transferring from the antenna bodies to the air and vice versa. As the total amount of heat must be preserved, the difference between the fluxes in the two opposite directions should be equal to zero.

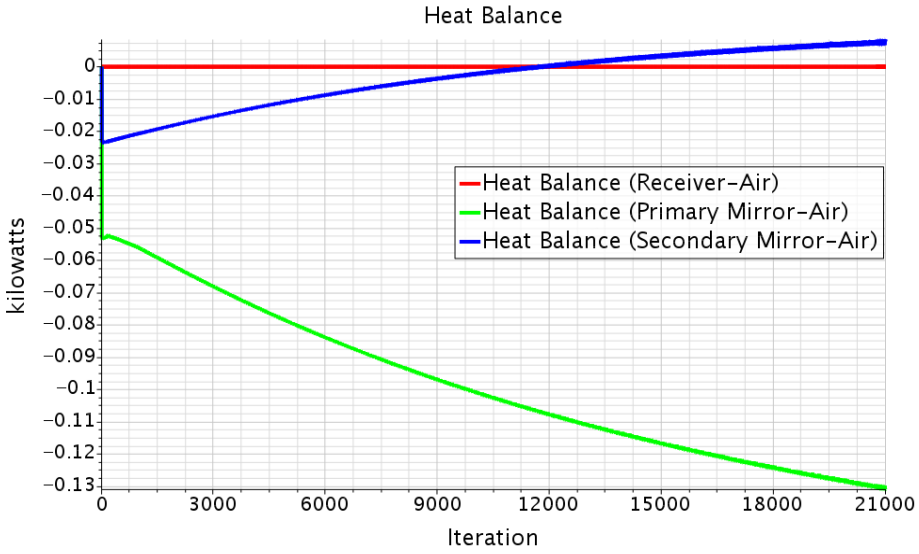

Figure 19 Net heat flux between the solid parts of the antenna and the air (wind at 3 m/s, Sun's altitude at 70°)

From the graph it is noticeable that the heat balance is not null for the mirrors, with an increasing absolute value for the primary mirror. However, the discrepancy is small if compared to the total amount of flux shown in Figure 18– with a proportion of about three orders of magnitude – and can hence be associated to a computational feature.

6.2 Solar position at 90° of altitude

The temperature fields for the two configurations in which the Sun has an altitude of 90° are shown below. Like in the previously treated situation, 21000 iterations were achieved for the case where the antenna symmetry axis is aligned with the z direction. In the other case only 4000 iterations were achieved, and the thermal features were investigate by comparing it with the other configuration.

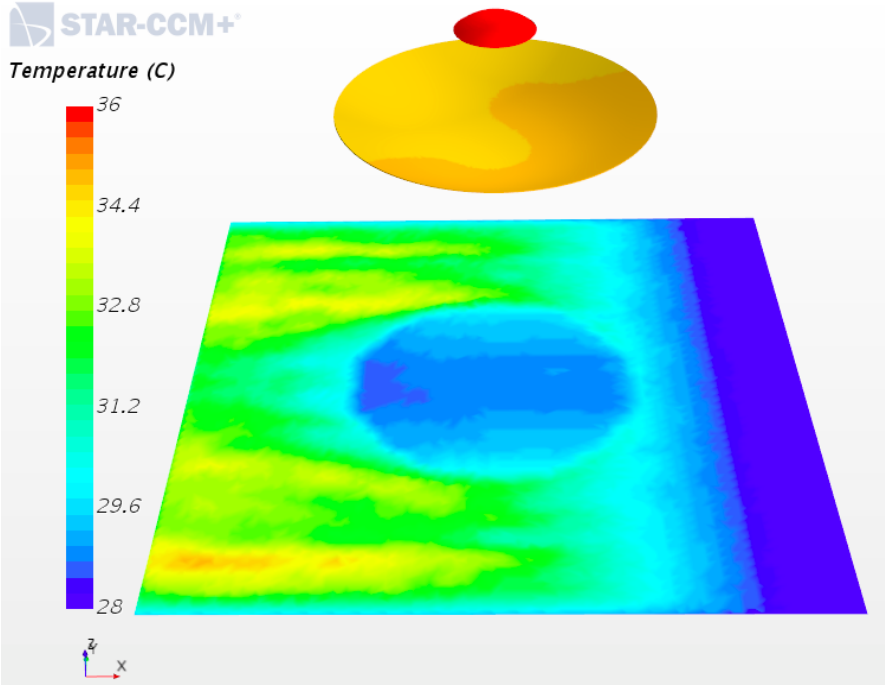

Figure 20 Temperature field of the system for a wind of 3 m/s and a Sun's altitude of 90°.

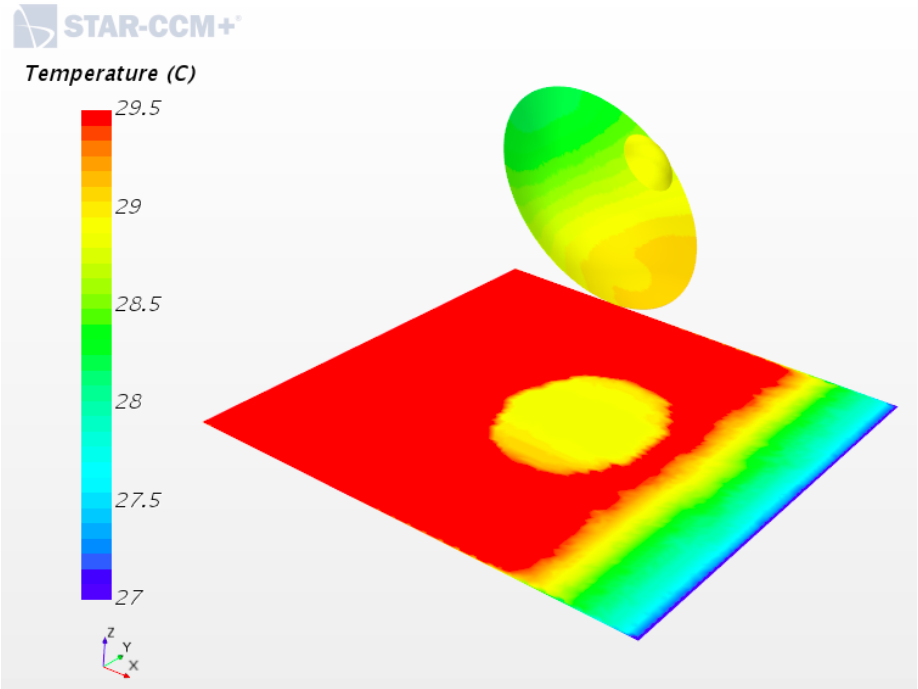

Figure 21 Temperature field of the system for a wind of 3 m/s and a Sun's altitude of 90°: the antenna is rotated of 45° towards the incoming wind

The trend of the maximum temperature reached by the mirrors and the receiver is shown below for both the antenna positions (Figure 22 and Figure 23). Few differences can be observed with respect to the previously treated situation of the Sun at 70° of altitude.

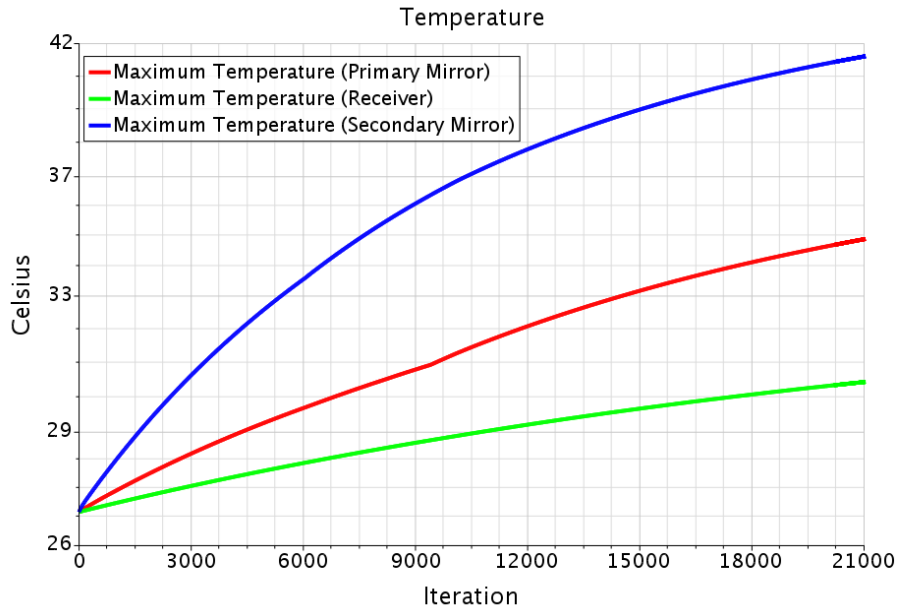

Figure 22 Temperature in solid structures in case of antenna symmetry axis aligned with z direction (wind at 3 m/s, Sun's altitude at 90°)

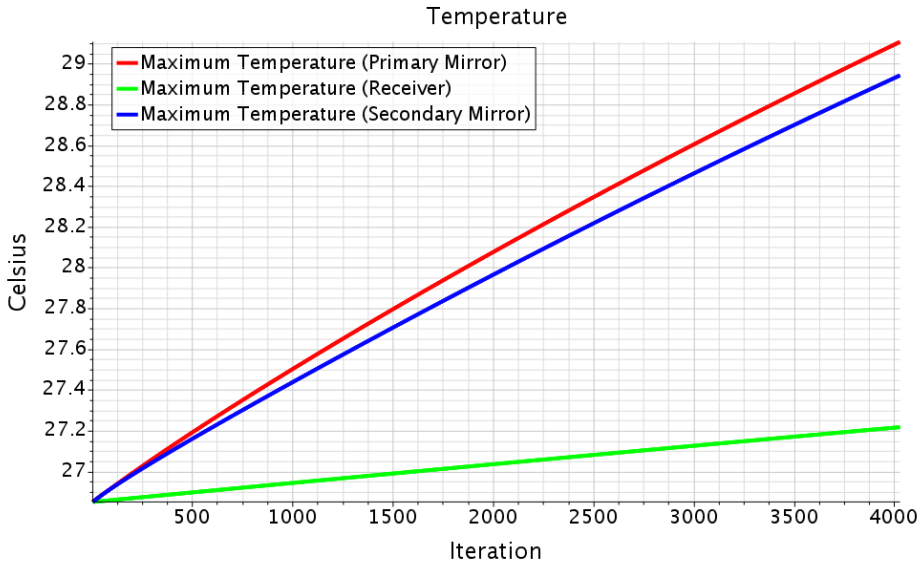

Figure 23 Temperature of solid structures in the case with the antenna rotated of 45° toward the wind (wind at 3 m/s, Sun's altitude at 90°)

The observed temperature in the first configuration is higher if compared to the case with the Sun at 70°. While the value at the receiver shows an increase of about 2°C and at the primary mirror the value is nearly identical, the most dramatic change is noticeable for the secondary mirror, for which the temperature reaches 42 °C, increasing of about 15 degrees with respect to the initial conditions settings. This difference may be explained by the different incidence angle of the direct irradiation arriving on the secondary mirror. Despite the higher

values, the trend of the three functions suggests the approaching to convergence.

In the second configuration with the rotated antenna the trend is similar but the slope is lower, which may suggest the achievement of convergence in a fewer number of iterations. While the temperature at the primary mirror does not vary considerably, at the secondary mirror and at the receiver its value is noticeably lower if compared to the configuration with the antenna aligned with the Sun's direction. Such result is also obtained by comparing the temperature value of the last case with the first investigated one (with a Sun's altitude of 70°).

The velocity field on a section across the air was recorded together with the temperature field on the ground for the last configuration. The results are shown is the successive images illustrated in Figure 24.

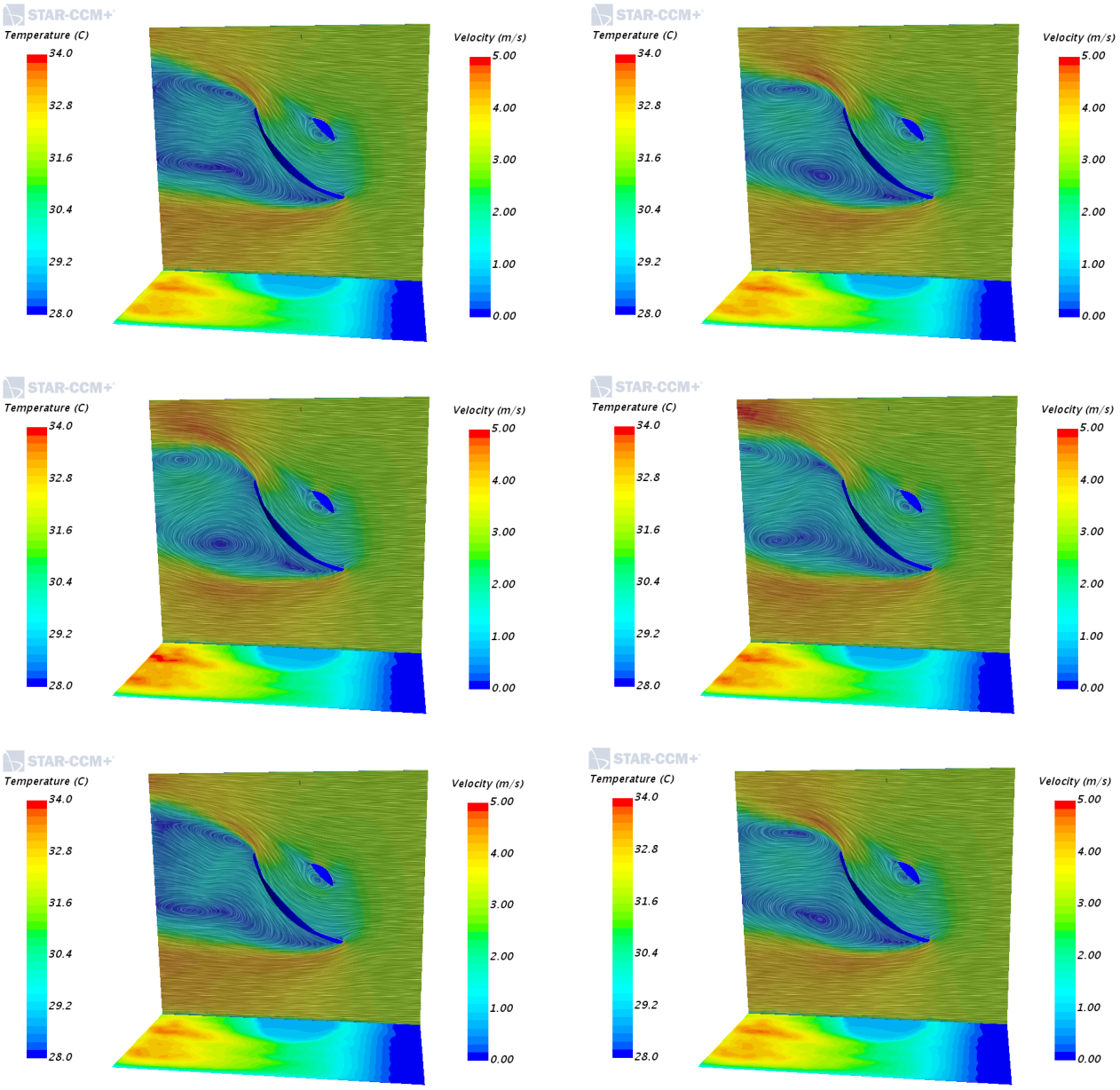

Figure 24 Temperature and velocity field of the antenna system with the Sun's position at 90°.

7 Thermal stress analysis

In the last part of the stage, the fundamentals for the a thermal stress analysis of the structure were investigated. As guideline for the application of the stress analysis, a tutorial exercise, *Thermal Strain: Exhaust Manifold*, was performed.

The simulation includes both conjugate heat transfer (CHT) and stress analysis. In STAR-CCM+, it is possible to combine the advantages of the finite volume (FV) and the finite element (FE) methods together in the same simulation. In the first part of the simulation, the steady-state temperature distribution throughout the solid domain is computed in a finite volume conjugate heat transfer analysis. In the second part of the simulation, the temperature data is mapped onto a finite element model of the solid structures for stress analysis.

As we are looking for the static/steady-state solutions in the fluid and the solid, it is both convenient and accurate to initially solve for the fluid flow and the conjugate heat transfer, and then solve for the solid displacement while holding the thermal field fixed.

The simulation strategy, including the model geometry and assumptions, is summarized below in Table 3 and Table 4.

Table 3 Summarized description of the thermal analysis

	Solid domain	Fluid domain
Geometry	Antenna	External volume around the solid domain
Assumptions and Models	Material: Al Equation of state: Constant density	Material: Air Equation of State: Ideal Gas Flow Regime: Turbulent
Boundary Conditions	Thermal specification for boundaries	Temperature at inlet Velocity at inlet
Type of Analysis	Steady	Steady
Discretization and Solution Method	Finite Volume (FV)	Finite Volume (FV)
Mesh	Polyhedral Cells	Polyhedral Cells

Table 4 Summarized description of the stress analysis

	Solid domain
Geometry	Antenna
Assumptions and Models	Material: Al Constitutive Law: Linear Elastic Geometry: Linear
Boundary Conditions	Constraints: Three point constraints Thermal Loads: Temperature Loads are calculated during thermal analysis and then mapped onto the FE mesh
Type of Analysis	Static
Discretization and Solution Method	Finite Element (FE)
Mesh	Tetrahedral Elements

Since the geometrical model created in the framework of this stage is a raw approximation of the main parts of a radio telescope, the results that can be obtained in this work may differ from the realistic values of stress to which the structure is subject; two of the most important differences are in particular the mirrors thickness and the surface continuity of the mirrors.

As a new physics continuum and new regions must be created for the solid structures in order to insert the stress models that account for the solid displacement in response to thermal loads, the first issue cannot be solved by modifying the material parameters as previously done in the continua section for the heat transfer description.

The second issue refers to the discrepancy with the real situation, in which the mirrors are divided into a great number of panels: this configuration in fact minimizes the strains applied to the structure. Moreover, following the tutorial indications it is necessary to apply constraints at vertices to avoid the rotation of the structure. However, as the mirrors surface is continuous, only few points are available and mirrors were fixed only by two points located at the parabola vertices on the internal and external surfaces.

Aiming to carry out a more realistic stress analysis, we can indicate that the following steps should be applied.

A surface slice should be cut from the mirrors in order to obtain a panel; as its dimensions would be decreased, the thickness may be reduced to the real value with less constraints originating from the mesh operations. The panel can be hence fixed in four points – in a way that is similar to the real fastening through actuators – and pressure and temperature fields are applied to the upper and lower surfaces from the fields that are mapped on the previous structure (the one used for the thermal analysis). Maintaining the approximate model used since this section, it is also possible to calculate the displacements which are parallel to the surfaces (which values may be close to the real ones, while in the vertical direction the difference is considerable) by finding the stress tensor elements.

In Figure 25 and Figure 26 the displacements obtained for the two configurations with the vertical axis of the antenna aligned with the z direction are shown.

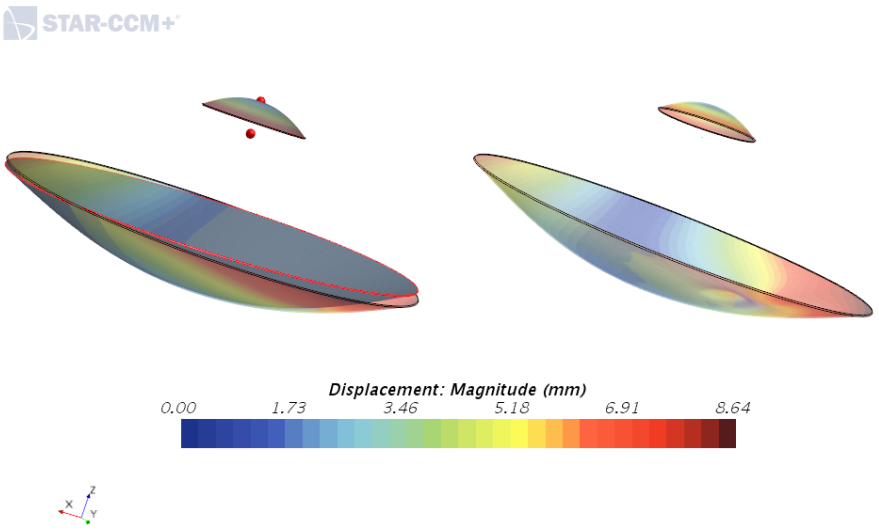

Figure 25 Displacement magnitude obtained with the thermal loads related to the configuration with the Sun at 70°

Displacements are enhanced through the addition of a Vector Warp derived part, in which the scale factor was set to 200. In the left image of each figure, the geometry parts of the system were overlapped to the displacements map in order to visualize the initial structural shape.

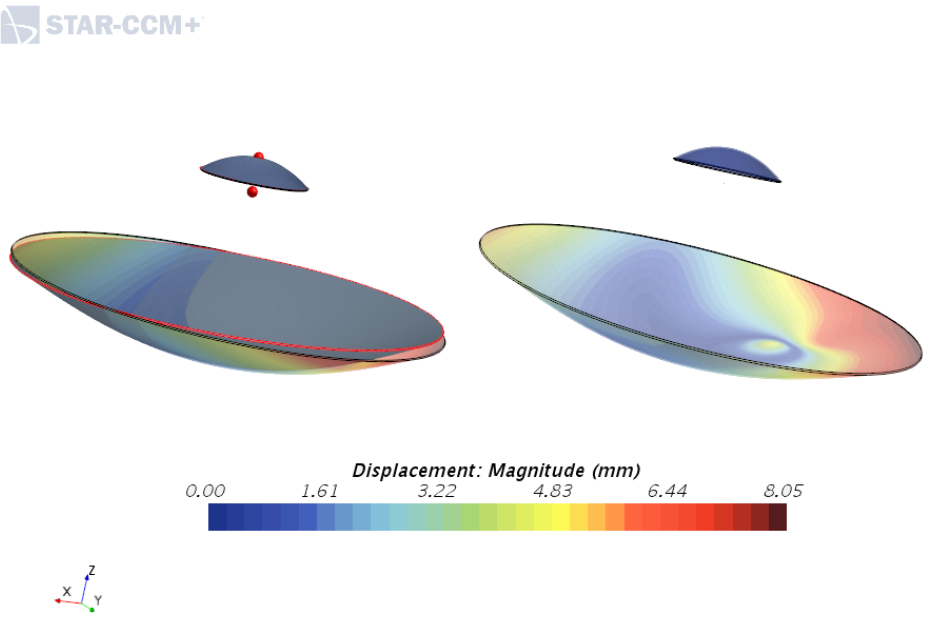

Figure 26 Displacement magnitude obtained with the thermal loads related to the configuration with the Sun at 90°

As seen from the figures above, the displacement obtained have a similar magnitude in both configurations: this may be related to the constrained applied more than the different thermal field from one case to the other.

8 Conclusions

The slow evolution of a simple and approximate model for a radio telescope via the consecutive addition of more complex features has been a fundamental process to reach a deep awareness on the characterization of a physical structure and evaluate the computational limits of the software, as reported in the previous chapters. Despite its simplicity, it has been possible to analyze various aspects of the system from the mechanical and thermal point of view with satisfying accuracy.

This experience is meant to provide a solid base for future development of the model, in which the geometry structure may be expanded and refine in order to carry out a more realistic analysis, especially from the mechanical and thermal stress analysis point of view.

References

1. Bolli P., Orlati A., Stinghetti L., et al., *Sardinia Radio Telescope: General Description*, Technical Commission and First Light, Journal of Astronomical Instrumentation, 2016.
2. http://www.crs4.it/research/energy-and-environment/
3. http://www.cd-adapco.com/
4. *Surface-to-Surface Radiation: Thermal Insulator* tutorial
5. *Thermal Strain: Exhaust Manifold* tutorial